Dissipative Circuit Quantum Electrodynamics

Resistive systems from reactive elements

Master thesis

Written by *Magnus Staal Vigsø*

May 21, 2024

Supervised by
Jens Paaske

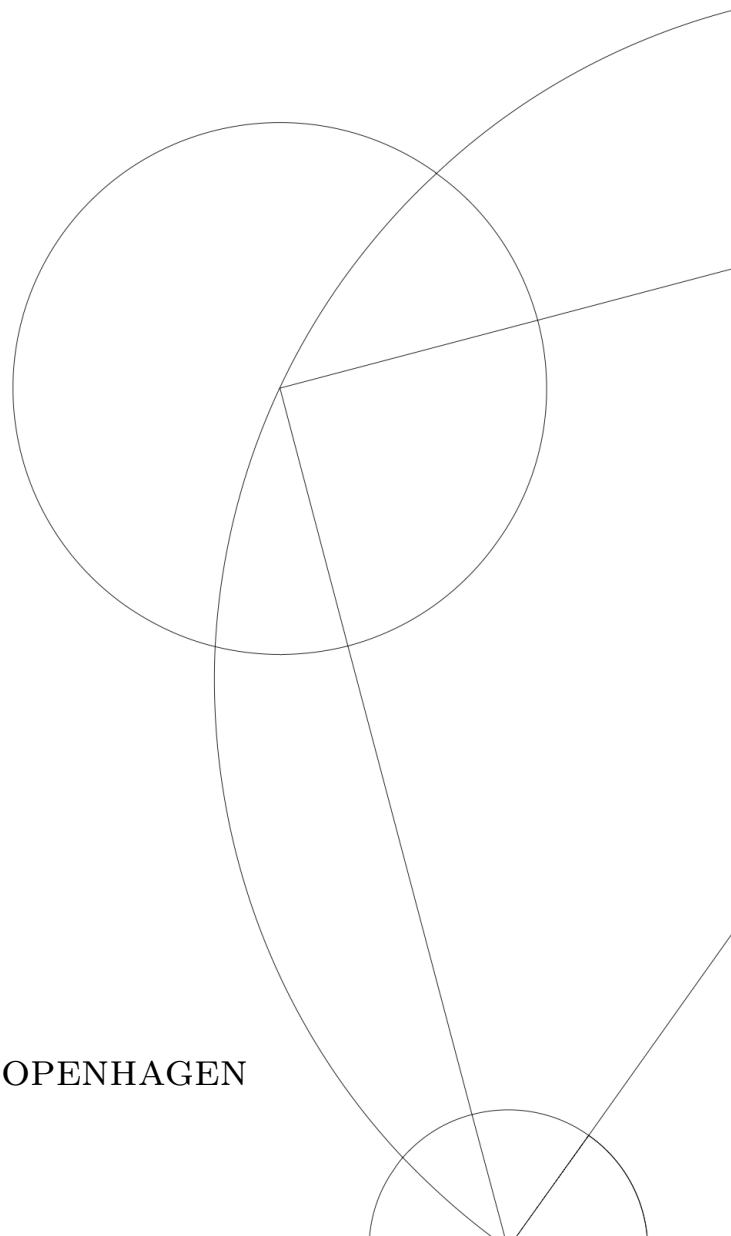

University of Copenhagen

UNIVERSITY OF COPENHAGEN

Name of Institute:	Niels Bohr Institute
Name of Department:	CMT
Author(s):	Magnus Staal Vigsø
Email:	zxb933@alumni.ku.dk
Title and subtitle:	Dissipative Circuit Quantum Electrodynamics - Resistive systems from reactive elements
Supervisor(s):	Jens Paaske
Handed in:	May 21. 2024
Defended:	N/A

Name _____

Signature _____

Date _____

Table of content

List of Figures

Abstract

Classical circuit theory is justified from the underlying laws of electrodynamics, and used to derive the Johnson-Nyquist noise correlation for the classical damped resonator circuit as an example of the fluctuation-dissipation theorem. Beginning with the quantization of a the undamped resonator, the method of nodes is introduced as a framework for performing circuit QED for circuits. It is shown that an excited boson mode decaying into a finite reservoir will experience Poincaré recurrences. This motivates the derivation of a Heisenberg-Langevin equation for the flux of a resonator circuit coupled to an infinite transmission line serving as a thermal bath. The bath degrees of freedom are solved exactly in the Heisenberg picture, and shown to subject the system to dissipation and fluctuations with memory effects. In the continuum limit, the spectral density of the bath is shown to obtain a Drude form. The symmetrized quantum noise correlation function is derived and shown to be another example of the fluctuation-dissipation theorem, as well as exhibiting zero-point fluctuations at low temperature. Finally, the continuous transmission line reservoir with Drude damping is shown to be the quantum description of the RC-circuit through a comparison of Fourier space response functions.

Acknowledgements

I sincerely thank my supervisor, Jens, for his careful guidance and great patience. He went above and beyond in guiding me through my thesis, even when I pushed his open-door policy to its limits.

I would also like to extend my thanks to my office mates, Hans, Yongtao and Yi, for providing great company and the occasional help during the writing process. Writing a thesis with the condensed matter theory group has been great. Many of its members have lent their aid and given valuable input to the various problems I have faced when writing this thesis.

Last, but not least, I am grateful for my family, who have supported me throughout my studies.

Chapter 1

Introduction

Dissipation of energy is ubiquitous in ordinary experience. Electronics get hot, spinning tops all eventually stop and anyone who has played on a swing knows the basic principle of a damped pendulum. For all intents and purposes, continued effort is required for continued motion. The widespread presence of frictional forces led Aristotle to assume a proportionality between force and velocity, rather than force and acceleration [39]. After the arrival of Newton's laws of motion, dissipation was correctly identified as various velocity-dependent forces such as Stoke's drag and surface friction. This concept of friction is also present in the world of electronics, where Ohm's law describes the dampening that the movement of charges experience when flowing through a conductor. A shared property of these non-conservative equations of motion is that all are derived empirically. Any attempt at deriving dissipative equations of motion in analytical mechanics will fail without techniques like the Rayleigh dissipation function [28], which does not follow from energy considerations, but rather an a priori intention of including dissipative forces. Unfortunately, such methods are not available in the theory of quantum mechanics. This poses a serious problem, as the time evolution of a quantum system is determined by a quantized Hamiltonian via the Schrödinger equation. To make matters worse, the fluctuation-dissipation theorem implies that random fluctuations will accompany any dissipative effects [7], as both phenomena have their origin in the system exchanging energy with an environment, making any open system inherently stochastic. For classical systems, this is not a problem. Dissipative effects are readily included through the aforementioned empirical laws, and the statistical properties of noise can be determined to allow numerical solutions of system trajectories [29]. As will be shown in this thesis, similar descriptions of a quantum system demands an explicit inclusion of a so-called reservoir which has a Hamiltonian of infinite degrees of freedom to accommodate one-way flow of energy from system to environment.

The framework of circuit quantum electrodynamics (circuit QED) allows great free-

dom in designing Hamiltonians of quantum systems which directly correspond to circuit diagrams [18]. Here the conventional variables of position and momentum for Hamiltonian systems are replaced by flux and charge, from which the Hamiltonian can easily by converted to a *circuit photon* basis in second quantization. In the same manner, a Hamiltonian in second quantization can be transformed back to the "classical" basis of flux and charge, which enables direct comparisons between quantum circuits and their classical counterparts. The purpose of this thesis is first to establish circuit theory as a means of analysing the dynamics of electrical systems, then derive the connection between dissipation and stochastic fluctuations in classical systems with the damped resonator circuit as the canonical example. Afterwards circuit QED is used to derive a microscopic Hamiltonian of infinite degrees of freedom for a quantum circuit-reservoir system, which is shown to exhibit both dissipative and stochastic behavior. Finally, the dissipative quantum circuit is given a classical analogue which displays the same dynamics to reach a direct correspondence between the fundamental quantum theory and the observed noisy-dissipative dynamics of classical systems. Along the way, fundamental concepts in dissipative quantum mechanics such as thermal reservoirs and their spectral densities are introduced, in addition to a study of the rotating-wave approximation as it is applied in circuit QED.

Outline of thesis

The sections of this thesis are structured as follows

- Chapter 2: Classical circuit theory is derived from the fundamental Maxwell equations governing the underlying electromagnetic fields. The equations of motion and stored energies of passive circuit components are expressed in terms of flux and charge, along with an introduction to Kirchhoff's circuit laws, Ohm's law of resistance and the more general concept of circuit impedance as a circuit's response function. With these, the theory of Brownian motion is adapted to the example of an RLC circuit subjected to Johnson-Nyquist noise, with a fluctuation-dissipation theorem derived from the circuit's response function. The final section of this chapter is a short treatment of the application of analytical mechanics in deriving the equations of motion for electrical circuits, with the resulting exclusion of Ohm's law serving as the motivation to introduce the thermal reservoirs as a way of including dissipative effects in Hamiltonian systems.

- Chapter 3: The textbook quantum harmonic oscillator is introduced in the form of a quantized LC resonator circuit, along with the bosonic creation and annihilation operators of circuit photons as they appear in circuit QED. Afterwards

the method of nodes is introduced as the analytical tool of choice for obtaining the Hamiltonian and normal modes of circuits. Using this method, the dispersion relation is derived for three systems: two resonators sharing a capacitor, a transmission line in the continuum limit and one which is kept discrete. For the system with a capacitive coupling and the discrete transmission line, the effects of neglecting the Hamiltonian's particle non-conserving terms on the dispersion relation is examined. Afterwards an attempt is made at including an environment in the Schrödinger equation using a finite-sized thermal reservoir for a single particle moving between bosonic modes. Finally, the inevitable Poincaré recurrences of finite systems are observed in the Schrödinger equation solution, which motivates the final chapter on preventing Poincaré recurrences using a reduced system-environment description for an infinite reservoir.

- Chapter 4: An equation motion for the node flux of a resonator circuit coupled to an infinite transmission line is derived in the Heisenberg picture by solving the bath modes exactly. The infinite reservoir is shown to add a velocity-dependent friction term with memory and a stochastic noise term to the flux equation of motion. The result is a Langevin equation for a quantum operator in the Heisenberg picture. Afterwards, the concept of a spectral distribution and density for characterizing the dissipative properties of reservoirs is introduced, along with some of their physically motivated mathematical properties. Afterwards an analytical expression of the transmission line's response function is derived, and it is shown that taking the continuum limit of the transmission line yields a dissipation with an exponentially decaying memory. The noise correlation function is then derived, and it is directly seen how dissipation and fluctuations are directly related as the reservoir is now explicitly included in the system description. The chapter concludes by revealing the RC-circuit as the classical counterpart of the continuous transmission line reservoir through inspection of the response function of each system.

Chapter 2

Classical Electronic Circuits and Noise

In this section, the framework used to analyze the dynamics of electrical circuits will be presented and justified. The Maxwell equations form the basis of this framework, and these will be used to derive Kirchhoff's circuit laws for a lumped-element model of circuits.

Ampere's law relates the total current I passing through a component b (also referred to as a *branch*) to the closed line integral of the B-field outside it which encloses said component [35]

$$I_b(t) = \frac{1}{\mu_0} \oint_b \vec{B} \cdot d\vec{\ell} \tag{2.1}$$

The voltage drop across b is defined as going in the opposite direction as that of the current I_b and the electromotive force $\mathcal{E}$. Specifically the voltage is defined as the line integral across the electric field inside a component going from one end to the other

$$V_b(t) = -\mathcal{E}_b(t) = \int_{\text{start of } b}^{\text{end of } b} \vec{E}(t) \cdot d\vec{\ell} \tag{2.2}$$

Whenever current or voltage is used in this thesis, know that the field equations (2.1) and (2.2) relate any circuit dynamics to the underlying theory of electrodynamics. The reason for not using direct calculations of the electromagnetic fields is the difficulty that these pose for even comparatively simple systems. Instead the *lumped-element* model of circuits is applied. Here, the physical dimensions of the system is reduced to an abstract diagram of components connected with lossless wires. The dynamics of the electrical system then loses its dependence on its spacial configuration, and can be described by purely time-dependent quantities such as current and voltage.

This idealization of reality does have its limits however, as the wave nature of electromagnetism can not be ignored if the physical dimensions of the circuit reach a considerable fraction of its electrical wavelength. In such cases one must instead apply a *transmission line* description to bridge the gap between circuit theory and electrodynamics [34]. Transmission lines allow spatial variations in voltage and current, and will be described further in section 3.3. While voltage and current work fine as the dynamical quantities for classical circuits, flux and charge is better suited for the formalism that is used in the analysis of quantum circuits. Branch charge simply follows from integrating current in time

$$Q_b(t) = \int_{-\infty}^{t} I_b(t')dt' \tag{2.3}$$

Similarly, branch flux follows from integrating Faraday's law of induction [35]

$$\Phi_b(t) = -\int_{-\infty}^{t} \mathcal{E}_b(t')dt' = \int_{-\infty}^{t} V_b(t')dt' \tag{2.4}$$

Where the lower integration bound of both is set to $t' = -\infty$, as the system can be assumed to be at rest in the infinite past [37]. With the dynamical quantities of circuit analysis established, the circuit components used in this thesis can now be introduced.

2.1 Reactive circuit components

The capacitor

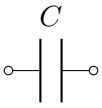

Figure 2.1.1: Circuit diagram representation of a linear capacitor with capacitance C.

An isolated conductor carrying charge Q will have the electric potential φ_0 which goes to zero at infinity [35]. These two quantities are related by the *capacitance* C of the conductor. For two plates carrying opposite charges in close proximity, edge variations can be neglected and the small nonlinearities that make C a function of charge and electric potential can be ignored. The result is a linear relation between capacitor voltage and stored charge determined by the constant C

$$\varphi_1(t) - \varphi_0(t) = V(t) = \frac{Q(t)}{C} \tag{2.5}$$

The circuit symbol of which can be seen on Fig. 2.1.1. The branch flux of a linear capacitor follows from the time derivative of Eq.(2.4). The flux-charge relation of the capacitor is then

$$\dot{\Phi}(t) = \frac{Q(t)}{C} \tag{2.6}$$

Though capacitors do not allow an actual flow of electrons through them, the time derivative of capacitor charge still functions as an effective current through the capacitor. The relation between charge, current and branch flux is therefore

$$C\ddot{\Phi}(t) = I(t) = \dot{Q}(t) \tag{2.7}$$

Lastly, the energy stored in a capacitor can be found as the integral of the power $P(t) = V(t)I(t)$ integrated from $t' = -\infty$ to t

$$E_C(t) = C\int_{-\infty}^{t} \dot{\Phi}(t)\ddot{\Phi}(t) = \frac{C}{2}\dot{\Phi}(t)^2 = \frac{1}{2C}Q(t)^2 \tag{2.8}$$

The Inductor

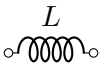

Figure 2.1.2: Circuit diagram representation of a linear inductor with inductance L.

Faraday's law gives the relation between a changing magnetic flux and the induced electromotive force (emf)

$$\mathcal{E}(t) = -\dot{\Phi}(t) \tag{2.9}$$

For a linear inductor, the relation between current and magnetic flux is given by the constant *inductance* L

$$\Phi(t) = LI(t) \tag{2.10}$$

From the two above equations it can be seen that the voltage drop across a linear inductor must be

$$-\mathcal{E}(t) = V(t) = \dot{\Phi}(t) = L\dot{I}(t) \tag{2.11}$$

The energy stored in a linear inductor is again found by integrating the product of its branch current and voltage from Eqs. (2.10) and (2.11)

$$E_L(t) = \frac{1}{L}\int_{-\infty}^{t} \Phi(t)\dot{\Phi}(t) = \frac{1}{2L}\Phi(t)^2 \tag{2.12}$$

With charge-flux relations and expressions for stored energy derived for capacitors and inductors, the next step to performing circuit analysis is finding the laws governing a circuit's equation of motion.

2.2 Classical circuit laws and impedance

Kirchhoff's voltage law

Kirchhoff's voltage law follows directly from Faraday's law of induction. Any loop which is not subjected to an external magnetic flux must have a vanishing sum of voltage drops. Mathematically, a loop $\mathcal{C}$ of components $b_1, b_2, \ldots, b_N$ must satisfy the following sum rule

$$\oint_{\mathcal{C}} \vec{E} \cdot d\vec{\ell} = \int_{\text{start of } b_1}^{\text{end of } b_1} \vec{E} \cdot d\vec{\ell} + \int_{\text{start of } b_2}^{\text{end of } b_2} \vec{E} \cdot d\vec{\ell} + \cdots + \int_{\text{start of } b_N}^{\text{end of } b_N} \vec{E} \cdot d\vec{\ell} = \sum_{i}^{N} V_i = 0 \quad (2.13)$$

This law allows the derivation of an equation of motion for any loop of electrical components.

Kirchhoff's current law

Kirchhoff's current law can be found by considering continuity equation

$$\oint_S \vec{J} \cdot d\vec{S} = -\frac{\partial}{\partial t} \int_V \rho dV \quad (2.14)$$

Where $\vec{J}$ is the current vector, ρ the charge density, S the surface and V the volume of some system. By applying this relation to a circuit node connecting N branches with N_C being capacitors, the left-hand term must be the sum of conductive currents entering and leaving the node, while the right-hand side is the time derivative of accumulated charge on said node

$$\sum_{i}^{N-N_C} I_i = -\dot{Q} \quad (2.15)$$

Kirchhoff's current law is obtained by interpreting the time derivative of charge on the node as a capacitive current to be included among the conductive currents [36]

$$\sum_{i}^{N} I_i = 0 \quad (2.16)$$

Ohm's law

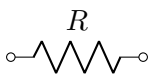

Figure 2.2.1: Circuit diagram representation of an Ohmic resistor with resistance R.

Finally, Ohm's law is used to include dissipative terms in the dynamics of circuits. It predicts a linear relation between an electric potential difference V along a conductor and the current I which runs through it. The ratio of V and I is given by the resistance in units of ohm (Ω).

$$\frac{V(t)}{I(t)} = R \tag{2.17}$$

In circuit theory, this law is used to include the voltage drop of Ohmic resistors (See Fig. 2.2.1) in Kirchhoff's voltage law.

Impedance

The equations of motion for multicomponent circuits can become very complicated. Luckily the dynamics of circuits can be simplified into a frequency representation of Ohm's law by using the *Fourier transformation*[1]. The resulting ratio between $V(\omega)$ and $I(\omega)$ still in units of Ω, but is now a complex number referred to as the circuit *impedance* Z. The impedance of the capacitor is found by differentiating its voltage drop (2.6) and bringing it to the form of Ohm's law (2.17) by inserting the frequency representation of $V(t)$ and $I(t)$ using Eq.(A.1)

$$Z_C = \frac{V(\omega)}{I(\omega)} = -\frac{1}{i\omega C} \tag{2.18}$$

The impedance of the inductor is found in the same fashion using Eq. (2.11)

$$Z_L = -i\omega L \tag{2.19}$$

and the impedance of the resistor is equivalent to its resistance

$$Z_R = R \tag{2.20}$$

The combined effective impedance of two components can be found by adding them together in the same manner as resistors

$$\begin{aligned} Z_{total} &= Z_1 + Z_2, \quad \text{For impedances connected in series} \\ Z_{total} &= \frac{1}{\frac{1}{Z_1} + \frac{1}{Z_2}}, \quad \text{For impedances connected in parallel} \end{aligned} \tag{2.21}$$

The real part of the impedance is the resistance, while the imaginary component is referred to as the *reactance* and constitutes a non-dissipative opposition to a time varying current.

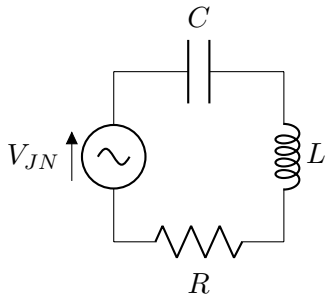

Figure 2.3.1: An RLC resonator circuit with capacitance C, inductance L and resistance R subjected to Johnson-Nyquist noise acting as stochastic voltage source.

2.3 The classical RLC circuit as a Langevin equation

The LC resonator is built by connecting an inductive coil in series with a capacitor. Summing together the voltage drops of the capacitor in Eq. (2.6) and the inductor in Eq. (2.11), one obtains the equation of motion of charge in the form of a harmonic oscillator

$$\ddot{Q}(t) = -\omega_0^2 Q(t) \tag{2.22}$$

Where $\omega_0 \equiv 1/\sqrt{LC}$ is the resonant frequency of the oscillator. Including resistance effects in the circuit will add a dissipative term to the above equation. This term is simply Ohm's law from Eq.(2.17)

$$\ddot{Q}(t) = -2\gamma\dot{Q}(t) - \omega_0^2 Q(t) \tag{2.23}$$

With $\gamma \equiv \frac{R}{2L}$ being the *attenuation*. The work of Johnson and Nyquist shows that fluctuations in voltage happen in all electrical conductors in equilibrium at non-zero temperatures [21, 31]. To accommodate this, a stochastic voltage term can be added to the equation of motion [44]. This noise can be interpreted as an effectively stochastic voltage source coupled in series with the circuit. The circuit diagram for this model can be seen on 2.3.1.

$$\ddot{Q}(t) + 2\gamma\dot{Q}(t) + \omega_0^2 Q(t) = \eta_{JN}(t) \tag{2.24}$$

With $\eta_{JN}(t) \equiv V_{JN}(t)/L$ being the stochastic noise term perturbing the capacitor charge difference. This is an example of a stochastic system with *additive noise*[2] and is referred

[1] See appendix A.

[2] Another type of noise is *multiplicative noise* which is a stochastic term that scale with a function of the system. Such systems can not be written like 2.24 due to $\eta(t)$ being ill-defined, and one must instead use Itô calculus [29].

to as a *Langevin equation* in honor of Paul Langevin, who was the first to apply Newtonian mechanics in the analysis of Brownian motion [26]. Because of $\eta(t)$, the system trajectory can not be solved analytically with initial conditions. Instead, individual system trajectories can be simulated numerically from the properties of $\eta(t)$ and compared against analytic expressions of statistical quantities such as capacitor charge variance $\langle Q(t)^2 \rangle$. Nyquist calculated the variance in voltage of a conductor by assuming thermal equilibrium and invoking the equipartition theorem. The same procedure can be applied to the RLC circuit to find the equilibrium variance in $\Phi(t)$ and $Q(t)$. The capacitor and inductor energies in Eqs. (2.8) and (2.12) predict the following variances in thermal equilibrium

$$\langle Q^2 \rangle = Ck_BT, \quad \langle \Phi^2 \rangle = Lk_BT \tag{2.25}$$

Note that the circuit resistance does not appear in these expressions. Keep in mind that they are only predictions for the flux and charge variance of an *ensemble* of RLC circuits in thermal equilibrium, and say nothing on how such an ensemble evolves in time. Obtaining the ensemble time evolution instead demands that the statistical properties of $\eta(t)$, such as mean and time correlation, be determined, allowing numerical solutions to (2.24).

It is fair to assume that the statistical distribution of $\eta(t)$ has a mean of zero. If this was not true, a system at rest would have a non-zero voltage bias when averaged in time, which is nonphysical. The time correlation of $\eta(t)$ is derived from its *power spectrum* which is defined from the squared magnitude of its *windowed Fourier transform*[3]. The power spectrum of $Q(t)$ and $\eta(t)$ is found from Eq.(2.24)

$$I_Q(\omega) = \lim_{T\to\infty} \frac{1}{T} \frac{1}{|\omega_0^2 - 2i\omega\gamma - \omega^2|^2} |\eta_T(\omega)|^2 \equiv \frac{1}{|\omega_0^2 - 2i\omega\gamma - \omega^2|^2} I_\eta(\omega) \tag{2.26}$$

The power spectrum of $\eta(t)$ can be derived by relating Eqs. (2.25) and (2.26) through the *Wiener-Khinchin theorem* [24]

$$\langle Q^2 \rangle = Ck_BT = \int_{-\infty}^{\infty} \frac{d\omega}{2\pi} \frac{1}{|\omega_0^2 - 2i\omega\gamma - \omega^2|^2} I_\eta(\omega) \tag{2.27}$$

In addition to $\eta(t)$ having a vanishing mean, its distribution can also be assumed as Gaussian per the central limit theorem. With these assumptions $\eta(t)$ becomes *white noise* which has the property of a constant power spectrum [29]. The inverse Fourier transform can now be computed with the residue theorem [2]. By extending ω to the complex plane, a closed contour $\mathcal{C}$ can be defined along the real axis and extending into the upper complex plane in the shape of a semicircle of infinite radius as seen on figure

[3]See appendix A.

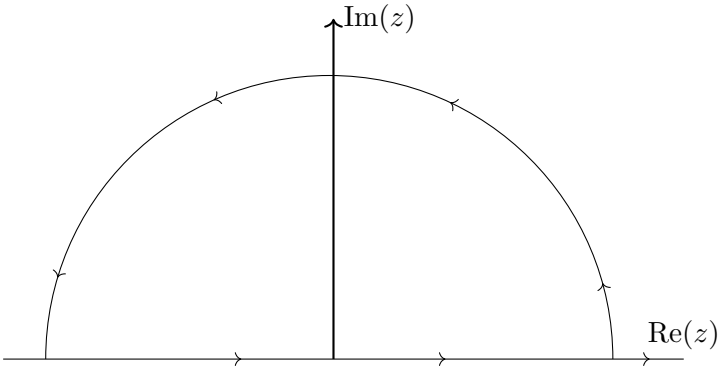

Figure 2.3.2: Counterclockwise contour integral containing the inverse Fourier transform of (2.27).

2.3.2. The resulting contour integral includes both (2.27) and a contribution from the semicircle path Γ in the complex plane

$$\oint_{\mathcal{C}} \frac{dz}{2\pi} \frac{1}{|\omega_0^2 - 2i\gamma z - z^2|^2} I_\eta = \int_{-\infty}^{\infty} \frac{d\omega}{2\pi} \frac{1}{|\omega_0^2 - 2i\gamma z - \omega^2|^2} I_\eta + \int_{\Gamma} \frac{dz}{2\pi} \frac{d\omega}{2\pi} \frac{1}{|\omega_0^2 - 2i\gamma z - \omega^2|^2} I_\eta \tag{2.28}$$

The contribution in the complex plane can be shown to vanish by using angular parameterization

$$\int_{\Gamma} \frac{dz}{2\pi} \frac{d\omega}{2\pi} \frac{1}{|\omega_0^2 - 2i\gamma z - \omega^2|^2} I_\eta = \lim_{r\to\infty} \int_0^{\pi} \frac{d\theta}{2\pi} \frac{i\theta r e^{i\theta}}{|\omega_0^2 - 2i\gamma r e^{i\eta} - r^2 e^{2i\theta}|^2} I_\eta = 0 \tag{2.29}$$

The inverse Fourier transform can then be performed by summing the residue of poles enclosed by the contour. The poles are easily found by writing the denominator in terms of the solutions to the quadratic equation $\omega_0^2 - 2i\gamma z - z^2 = 0$

$$\oint \frac{dz}{2\pi} f(z) \equiv \int_{\mathcal{C}} \frac{dz}{2\pi} \frac{1}{(z - z_-)(z - z_+)(z + z_+)(z - z_-)} I_\eta = i \left[\text{Res}(f, -z_-) + \text{Res}(f, -z_+)\right] \tag{2.30}$$

With $z_\pm \equiv -i\gamma \pm \sqrt{\omega_0^2 - \gamma^2}$. For non-critical damping $\omega_0 \neq \gamma$ there are two simple poles included in the upper complex plane at $z = -z_\pm$[4]. The physics of using these poles to evaluate the integral is the causality they impose, any system fluctuation must be in response to a force having acted in the past [30]. The associated residues are

$$\begin{aligned} \text{Res}(f, -z_+) &= \frac{I_\eta}{(-z_+ - z_-)(-z_+ - z_+)(z_- - z_+)} \\ \text{Res}(f, -z_-) &= \frac{I_\eta}{(-z_- - z_-)(-z_- - z_+)(z_+ - z_-)} \end{aligned} \tag{2.31}$$

[4]This is also the case in the overdamped regime $\omega_0 < \gamma$ where $\sqrt{\omega_0^2 - \gamma^2}$ is an imaginary number. As $i\sqrt{\gamma^2 - \omega_0^2}$ is guaranteed to be smaller than $i\gamma$ when $\omega_0 < \gamma$, it can not shift the poles across the real line.

The large amount of minus signs are cumbersome and the poles are redefined as $\omega_\pm = i\gamma(1 \pm \sqrt{1-\omega_0^2/\gamma^2})$

$$\text{Res}(f, -z_+) + \text{Res}(f, -z_+) = \frac{I_\eta}{2(\omega_+^2 - \omega_-^2)}\left[\frac{1}{\omega_+} - \frac{1}{\omega_-}\right] = \frac{I_\eta}{4i\gamma\omega_0^2} \tag{2.32}$$

Inserting this result into (2.27) and solving for I_η yields yields the power spectrum for η in thermal equilibrium

$$I_\eta = 4\gamma\omega_0^2 C k_B T \equiv 2\frac{k_B T}{L^2}R \tag{2.33}$$

Which means the power spectrum of the original fluctuating voltage V_{jn} is

$$I_{V_{jn}} = 2k_B T R \tag{2.34}$$

By applying the Wiener-Khinchin theorem once again, it can be seen that white noise necessarily implies a "memoryless" noise correlation function

$$\langle V_{JN}(t)V_{JN}(t')\rangle = 2k_B T R \int_{-\infty}^{\infty} \frac{d\omega}{2\pi} e^{i\omega(t-t')} = 2k_B T R\delta(t-t') \tag{2.35}$$

This relationship between voltage fluctuations and the resistance of the circuit is an example of a *fluctuation-dissipation theorem*. These types of relations are ubiquitous for lossy systems and show that fluctuations and dissipation are intrinsically related.

2.4 Hamiltonian Mechanics of electrical circuits

With a system Hamiltonian, analytical mechanics can provide an equivalent yet eloquent method of analysis to the application of Kirchhoff's and Ohm's laws. Using the LC circuit as the canonical example, one can write its Hamiltonian as the sum of Eqs. (2.8) and (2.12)

$$H = \frac{C}{2}\dot{\Phi}(t)^2 + \frac{\Phi(t)^2}{2L} = \frac{1}{2C}Q(t)^2 + \frac{1}{2}C\omega_0^2\Phi(t)^2 \tag{2.36}$$

Comparing this with the Hamiltonian of a 1D harmonic oscillator [19]

$$H = \frac{p^2(t)}{2m} + \frac{m\omega_0^2 x(t)^2}{2} \tag{2.37}$$

It can be seen that in electrical circuits, the charge $Q(t)$ can be interpreted as momentum and flux $\phi(t)$ as position. In addition, the capacitance C acts as the mass while the inductance is the inverse spring constant.

The canonical conjugates of the LC circuit must then be the charge Q and flux Φ of a component. Canonical conjugates are by definition each others Fourier transform and follow Hamilton's equations in classical mechanics [19]

$$\dot{\Phi} = \frac{\partial H}{\partial Q}, \quad \dot{Q} = -\frac{\partial H}{\partial \Phi} \quad \text{(Classical)} \tag{2.38}$$

In quantum mechanics, flux and charge satisfy the canonical commutation relation, which can be used in Heisenberg's equation of motion

$$[\hat{x}, \hat{p}] = [\hat{\Phi}, \hat{Q}] = i\hbar, \quad \dot{\hat{A}}_{(H)} = \frac{i}{\hbar}[\hat{H}, \hat{A}_{(H)}] \quad \text{(Quantum mechanical)} \tag{2.39}$$

While applying either Hamilton's or Heisenberg's equations will result in dynamics equivalent to Kirchoff's circuit laws for reactive components that have expression of energy, the fact that resistors do not have such an expression means that Ohm's law will be out of reach of any naive application of analytical mechanics or quantum mechanics. That is not to imply that resistors destroy energy, they do not. Instead the energy is converted to heat which flows into the environment, a process which is not included in lumped-element circuit analysis. With this in mind, the following chapter will apply the view of flux and charge as each others canonical conjugates to derive a description of circuits as quantum mechanical systems.

Chapter 3

Quantum Electronic Circuits

3.1 Quantizing the LC resonator

In quantum mechanics, variables like Q and Φ become operators. The quantized Hamiltonian is then:

$$\hat{H} = \frac{\hat{Q}^2}{2C} + \frac{C\omega_0^2\hat{\Phi}^2}{2} \tag{3.1}$$

The above expression can be brought into *second quantization*, where the energy is expressed in terms of bosonic photon excitations of the system. This is done by finding the *creation* and *annihilation operators* of the system. A systematic way of finding these is expressing the Hamiltonian as the product of $\hat{\Phi} - i\hat{Q}/\omega_0 C$ with its hermitian conjugate

$$\left(\hat{\Phi} - i\frac{\hat{Q}}{\omega_0 C}\right)\left(\hat{\Phi} + i\frac{\hat{Q}}{\omega_0 C}\right) = \hat{\Phi}^2 + \frac{\hat{Q}^2}{\omega_0^2 C^2} + i\frac{[\hat{\Phi}, \hat{Q}]}{\omega_0 C} \tag{3.2}$$

$$\hat{\Phi}^2 + \frac{\hat{Q}^2}{\omega_0^2 C^2} - \frac{\hbar}{\omega_0 C} = \frac{2}{\omega_0^2 C}\hat{H} - \frac{\hbar}{\omega_0 C}$$

By solving for the Hamiltonian

$$\hat{H} = \hbar\omega_0\left[\frac{\omega_0 C}{2\hbar}\left(\hat{\Phi} - i\frac{\hat{Q}}{\omega_0 C}\right)\left(\hat{\Phi} + i\frac{\hat{Q}}{\omega_0 C}\right) + \frac{1}{2}\right] = \hbar\omega_0\left(\hat{b}^\dagger\hat{b} + \frac{1}{2}\right) \tag{3.3}$$

The bosonic annihilation(creation) operator is obtained

$$\hat{b}^{(\dagger)} \equiv \sqrt{\frac{\omega_0 C}{2\hbar}}\left(\hat{\Phi} \pm i\frac{\hat{Q}}{\omega_0 C}\right) \tag{3.4}$$

Which follows the canonical commutation relation [38]

$$[\hat{b}, \hat{b}^\dagger] = \frac{1}{2\hbar}\Big(-i[\hat{\Phi}, \hat{Q}] + i[\hat{Q}, \hat{\Phi}]\Big) = 1 \tag{3.5}$$

From these the number operator can be defined

$$\hat{N} \equiv \hat{b}^\dagger \hat{b} \tag{3.6}$$

The name is justified by considering the Hamiltonian of the LC circuit in Eq. (3.3). Since $\hat{H}$ is a linear function of $\hat{N}$, both can be diagonalized simultaneously. The energy eigenkets of $\hat{N}$ are denoted by their eigenvalue n

$$\hat{N}|n\rangle = n|n\rangle \tag{3.7}$$

It is instructive to consider the commutator of $\hat{N}$ with $\hat{b}$

$$[\hat{N}, \hat{b}] \equiv [\hat{b}^\dagger \hat{b}, \hat{b}] = \hat{b}^\dagger [\hat{b}, \hat{b}] + [\hat{b}^\dagger, \hat{b}]\hat{b} = -\hat{b} \tag{3.8}$$

And likewise for $\hat{b}^\dagger$

$$[\hat{N}, \hat{b}^\dagger] = \hat{b}^\dagger \tag{3.9}$$

This implies

$$\hat{N}\hat{b}^{(\dagger)}|n\rangle = ([\hat{N}, \hat{b}^{(\dagger)}] + \hat{b}^{(\dagger)}\hat{N})|n\rangle = (n \mp 1)\hat{b}^{(\dagger)}|n\rangle \tag{3.10}$$

From which it is clear that $\hat{b}^{(\dagger)}|n\rangle$ is also an eigenket of $\hat{N}$. The eigenkets $\hat{b}^{(\dagger)}|n\rangle$ and $|n-1\rangle$ are therefore related by a constant, which by the normalization condition of $|n\rangle$ and $|n-1\rangle$ can be shown to be $\sqrt{n}$[38]. The effect of applying $\hat{b}^{(\dagger)}$ to the state $|n\rangle$ is then

$$\hat{b}|n\rangle = \sqrt{n}|n-1\rangle, \quad \hat{b}^\dagger|n\rangle = \sqrt{n+1}|n+1\rangle \tag{3.11}$$

Which is the justification of the terms *annihilation* and *creation* operator.

In summary, promoting the flux and charge functions to quantum mechanical operators allows one to recast the description of the LC circuit to one based on counting discrete photon excitations in the system. This is the basis for *circuit quantum electrodynamics*, as photon excitations result from the interaction of electrons in circuits. This formulation will later prove useful when computing certain equilibrium correlation functions, as the expectation number of non-interacting bosons follow the Bose-Einstein distribution function in thermal equilibrium.

3.2 Method of nodes

An alternate procedure to Kirchhoff's laws for determining the equations of motion for a circuit is the *method of nodes*. This method was proposed by Devoret [45, 37] and is useful for removing superfluous degrees of freedom, which becomes increasingly important with more complicated circuits. A *node* is defined as a point where two or more branches connect. From this, a *ground node* can be defined as the reference point of the remaining

nodes in regards to the electric potential. The ground node of a circuit is inactive as a result, and does not contribute to the dynamics to the system. The other nodes can then be grouped into *active* and *passive* nodes. An active node has at least one capacitor and one inductor connected to it, while the passive node only connects either capacitors or inductors. The distinction is important as passive nodes represent superfluous degrees of freedom, similar to how one can find an effective capacitance for a serial or parallel connection of capacitors. From the discussion in section 1, each component of a circuit will have a branch flux as the time integral of its voltage drop. The entirety of a circuit's branch fluxes can concisely collected into the *branch flux vector*

$$\mathbf{\Phi} = \begin{pmatrix} \Phi_1 \\ \vdots \\ \Phi_N \end{pmatrix} \tag{3.12}$$

All capacitors in a circuit constitute the a subset of branches, which are mutually related through the *capacitance matrix* $\boldsymbol{C}$ which is a result from classical electrostatics.

The Capacitance Matrix

For a lumped-element circuit, the capacitance between N nodes can be structured into a *mutual capacitance matrix*. This has the general form:

$$[C_m] = \begin{bmatrix} C_{m,11} & C_{m,12} & \dots & C_{m,1N} \\ C_{m,21} & C_{m,22} & \dots & C_{m,2N} \\ \vdots & \vdots & \ddots & \vdots \\ C_{m,N1} & C_{m,N2} & \dots & C_{m,NN} \end{bmatrix} \tag{3.13}$$

There is also the *Maxwell capacitance matrix*, which is derived from electrostatics. The uniqueness theorem states that the electric fields of a network of conductors is uniquely determined if given their potentials V_i [35]. From this follows the fact that the charge on each conductor is then also uniquely determined. This means that the charge of conductor i can be expressed as a linear combination of the potentials of the system times its coefficient of capacitance that makes up the capacitance matrix

$$\begin{pmatrix} Q_1 \\ Q_2 \\ \dots \\ Q_N \end{pmatrix} = \begin{bmatrix} C_{11} & C_{12} & \dots & C_{1N} \\ C_{21} & C_{22} & \dots & C_{2N} \\ \vdots & \vdots & \ddots & \vdots \\ C_{N1} & C_{N2} & \dots & C_{NN} \end{bmatrix} \begin{pmatrix} V_1 \\ V_2 \\ \vdots \\ V_N \end{pmatrix} \tag{3.14}$$

The Maxwell capacitance matrix expression for the charge on node i is then

$$Q_i = \sum_j^N C_{ij} V_j \tag{3.15}$$

While the mutual capacitance gives the charge as

$$Q_i = \sum_j C_{m,ij}(V_i - V_j) \tag{3.16}$$

By considering the coefficients of each electric potential, the Maxwell capacitance coefficients can be related to their mutual capacitance counterparts by

$$C_{ii} = \sum_j^N C_{m,ij} \tag{3.17}$$

$$C_{ij} = -C_{m,ij}$$

The Maxwell capacitance matrix expressed in terms of the circuit capacitances in the capacitive subgraph is then:

$$[C] = \begin{bmatrix} \sum_i C_{m,1i} & -C_{m,12} & \dots & -C_{m,1N} \\ -C_{m,21} & \sum_i C_{m,2i} & \dots & -C_{m,2N} \\ \vdots & \vdots & \ddots & \vdots \\ -C_{m,N1} & -C_{m,N2} & \dots & \sum_i C_{m,Ni} \end{bmatrix} \tag{3.18}$$

In the case of two nodes i and j not being connected through a capacitance, the corresponding capacitance matrix component will be zero. The *inductive matrix* $\left[L^{-1}\right]$ is constructed in a similar fashion, though with inverse inductances counted between nodes instead [37].

Equations of Motion

With this framework for relating the capacitance and inductance between nodes, one can begin finding the equations of motion through Eq. (2.8) and (2.12) by looking at the difference in flux between nodes. First, one defines a zero point reference node for flux, which will act as the ground for the circuit. The flux of the remaining nodes can then be collected into a vector

$$\boldsymbol{\phi} = \begin{pmatrix} \phi_1 \\ \phi_2 \\ \vdots \\ \phi_{n-1} \end{pmatrix} \tag{3.19}$$

For a system with n nodes. This vector is distinct from the vector in Eq. (3.12) which contains the fluxes in each *branch* of a system with N components. With the node flux vector, $[L^{-1}]$ and $[C]$ defined, the kinetic and potential energy can be found via

$$E_{kin} = \frac{1}{2}\dot{\boldsymbol{\phi}}^T \boldsymbol{C} \dot{\boldsymbol{\phi}} \tag{3.20}$$

$$E_{pot} = \frac{1}{2}\boldsymbol{\phi}^T \boldsymbol{L}^{-1}\boldsymbol{\phi} \tag{3.21}$$

With $\boldsymbol{C}$ and $\boldsymbol{L}^{-1}$ being $[C]$ and $[L^{-1}]$ though with the ground node removed like $\boldsymbol{\psi}$. This is done for the sake of brevity, as the ground node does not contribute to the dynamics of the circuit. From this the Lagrangian of the circuit can be found

$$\mathcal{L} = \frac{1}{2}\dot{\boldsymbol{\phi}}^T \boldsymbol{C}\dot{\boldsymbol{\phi}} - \frac{1}{2}\boldsymbol{\phi}^T \boldsymbol{L}^{-1}\boldsymbol{\phi} \tag{3.22}$$

From this, the node charge can be obtained as the conjugate momentum of the node flux [37]

$$q_n = \frac{\partial \mathcal{L}}{\partial \dot{\phi}_n} \tag{3.23}$$

Using the matrix formulation of the Lagrangian, this becomes $\boldsymbol{q} = \boldsymbol{C}\boldsymbol{\phi}$. A corollary to this, is the fact that $\dot{\boldsymbol{\phi}}$ can be expressed as a function of $\boldsymbol{q}$, if $\boldsymbol{C}$ is invertible. When this is the case, the Hamiltonian can be computed through the Legendre transform of the Lagrangian

$$H = \dot{\boldsymbol{\phi}}^T \boldsymbol{q} - \mathcal{L} = \frac{1}{2}\boldsymbol{q}^T \boldsymbol{C}^{-1}\boldsymbol{q} + \frac{1}{2}\boldsymbol{\phi}^T \boldsymbol{L}^{-1}\boldsymbol{\phi} \tag{3.24}$$

As the passive nodes of the capacitive subgraph per definition has $\frac{\partial H}{\partial \psi_n} = 0$, it can be inferred that any given circuit can at most have the same number of normal modes as the number of active nodes, not counting the ground node.

Applying the Euler-Lagrange equation to Eq.(3.22) it can be seen that the equations of motion is

$$\boldsymbol{C}\ddot{\boldsymbol{\phi}} = -\boldsymbol{L^{-1}}\boldsymbol{\phi} \tag{3.25}$$

Remembering the role of capacitance as mass and inductance as the inverse spring constant, it can be seen that a network of capacitors and inductors follows a matrix version of Hooke's law. For an invertible capacitance matrix, this can be recast into the familiar form

$$\ddot{\boldsymbol{\phi}} = -\boldsymbol{C^{-1}}\boldsymbol{L^{-1}}\boldsymbol{\phi} = -\boldsymbol{\omega}^2\boldsymbol{\phi} \tag{3.26}$$

The normal modes can then be found as the eigenvectors of $\boldsymbol{\omega}^2$, with the eigenvalues being the squared normal mode frequencies of the system.

3.3 Quantizing coupled resonators

Two resonators with capacitive coupling

As an instructive example of method of nodes, consider the coupling of two resonator circuits with a mutual capacitance C_g seen on figure 3.3.1. The Lagrangian of such a

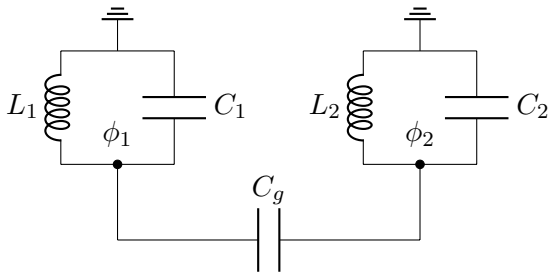

Figure 3.3.1: Two resonator circuits interacting through a shared capacitor, C_g.

setup in terms of node flux and charge can be written as

$$\mathcal{L} = C_1\frac{\dot{\phi}_1^2}{2} + C_2\frac{\dot{\phi}_2^2}{2} + C_g\frac{(\dot{\phi}_2 - \dot{\phi}_1)^2}{2} - \frac{\phi_1}{2L_1} - \frac{\phi_2}{2L_2} \tag{3.27}$$

With the basis $\boldsymbol{\phi} \equiv (\,\phi_1 \;\phi_2\,)^T$, the Lagrangian can be written in matrix form

$$\mathcal{L} = \frac{1}{2}\dot{\boldsymbol{\phi}}^T \begin{bmatrix} C_1 + C_g & -C_g \\ -C_g & C_2 + C_g \end{bmatrix} \dot{\boldsymbol{\phi}} - \frac{1}{2}\boldsymbol{\phi}^T \begin{bmatrix} \frac{1}{L_1} & 0 \\ 0 & \frac{1}{L_2} \end{bmatrix} \boldsymbol{\phi} \tag{3.28}$$

The Hamiltonian is found via a Legendre transformation by inverting $\boldsymbol{C}$ using the standard inversion procedure for a 2×2 matrix

$$\begin{aligned} H &= \frac{1}{2C_\Sigma^2}\boldsymbol{q}^T \begin{bmatrix} C_2 + C_g & C_g \\ C_g & C_1 + C_g \end{bmatrix} \boldsymbol{q} + \frac{1}{2}\boldsymbol{\phi}^T \begin{bmatrix} \frac{1}{L_1} & 0 \\ 0 & \frac{1}{L_2} \end{bmatrix} \boldsymbol{\phi} \\ &= C_2\frac{q_1^2}{2C_\Sigma^2} + C_1\frac{q_2^2}{2C_\Sigma^2} + C_g\frac{(q_1 + q_2)^2}{2C_\Sigma^2} + \frac{\phi_1^2}{2L_1} + \frac{\phi_2^2}{2L_2} \end{aligned} \tag{3.29}$$

With $\boldsymbol{q} \equiv \begin{pmatrix} q_1 & q_2 \end{pmatrix}^T$ and $C_\Sigma^2 \equiv C_gC_1 + C_gC_2 + C_1C_2$ being the determinant of $\boldsymbol{C}$. The basis can now be changed to that of circuit photons by promoting $\boldsymbol{q}$ and $\boldsymbol{\phi}$ to operators following canonical commutation (2.39) and inserting for the bosonic operators defined in (3.4). The resulting description is not of two oscillators "pushing and pulling" each other through a difference in charge, but an equivalent description of two bosonic modes exchanging photons with one another

$$\begin{aligned} \hat{H}/\hbar = \frac{\omega_1}{4}\left(\hat{b}_1^\dagger\hat{b}_1^\dagger + \hat{b}_1\hat{b}_1 + \hat{b}_1^\dagger\hat{b}_1 + \hat{b}_1\hat{b}_1^\dagger\right) + \frac{\omega_2}{4}\left(\hat{b}_2^\dagger\hat{b}_2^\dagger + \hat{b}_2\hat{b}_2 + \hat{b}_2^\dagger\hat{b}_2 + \hat{b}_2\hat{b}_2^\dagger\right) \\ +\omega_1\frac{C_2(C_1 + C_g)}{4C_\Sigma^2}\left(\hat{b}_1^\dagger\hat{b}_1 + \hat{b}_1\hat{b}_1^\dagger - \hat{b}_1\hat{b}_1 - \hat{b}_1^\dagger\hat{b}_1^\dagger\right) + \omega_2\frac{C_1(C_2 + C_g)}{4C_\Sigma^2}\left(\hat{b}_2^\dagger\hat{b}_2 + \hat{b}_2\hat{b}_2^\dagger - \hat{b}_2\hat{b}_2 - \hat{b}_2^\dagger\hat{b}_2^\dagger\right) \\ +\frac{C_g\sqrt{\omega_1\omega_2C_1C_2}}{2C_\Sigma^2}\left(\hat{b}_1^\dagger\hat{b}_2 + \hat{b}_1\hat{b}_2^\dagger - \hat{b}_1^\dagger\hat{b}_2^\dagger - \hat{b}_1\hat{b}_2\right) \end{aligned} \tag{3.30}$$

Whereas the Hamiltonian for an isolated resonator circuit simplifies to a single number operator with a constant energy shift, coupling the resonator to another yields a myriad of particle processes which no longer cancel each other. Of particular note are the terms composed entirely of either creation or annihilation operators. They denote particle non-conserving processes and are commonly referred to as *anomalous terms*. They often complicate the time evolution of the system, and it is therefore common to remove them in the so-called *rotating-wave approximation* (RWA).

In the interaction picture, one divides the Hamiltonian into two parts. The first part, $\hat{H}_0$, determines the time evolution of operators and is often called the *non-interacting* Hamiltonian. The second part, $\hat{V}$, determines the time evolution of the system state through the Schrödinger equation and is referred to as the *interaction Hamiltonian* [38]. A suitable choice of $\hat{H}_0$ allows an easy solution of the time evolution of operators, while potentially complicated interaction terms can be dealt with in perturbation theory, if need be. RWA is based on the time dependence obtained by the operators. Consider (3.3) in the interaction picture. For $\hat{H}_0 \equiv \omega_0 \hat{b}^\dagger \hat{b}$ the time evolution of $\hat{b}^{(\dagger)}$ can be found with the Baker-Hausdorff lemma [38]

$$\hat{b}^{(\dagger)}(t) = e^{i\hat{H}_0 t}\hat{b}e^{-i\hat{H}_0 t} = \hat{b} + i[\hat{H}_0, \hat{b}]t + \frac{1}{2!}i^2[\hat{H}_0, [\hat{H}_0, \hat{b}]]t^2 + \cdots = \hat{b}^{(\dagger)}e^{\mp i\omega_0 t} \tag{3.31}$$

Anomalous terms will therefore have a phase with the resonant frequency of its constituent modes added together, often resulting in the term oscillating rapidly. The RWA assumes that these oscillations cause the effect of anomalous terms on the system dynamics to average out in time [37]. This approximation is widespread in quantum optics and is often appropriated for use in circuit QED. As circuit QED allows one to relate a Hamiltonian to a corresponding circuit quantities, it will be instructive to examine what removing anomalous terms correspond to in the original basis of charge and flux. Writing the RWA Hamiltonian of fig 3.3.1 in second quantization and inserting (3.4) yields

$$\begin{aligned}\hat{H}_{\text{RWA}} = \hbar\frac{\omega_1}{4}\left(1 + \frac{C_1(C_2+C_g)}{C_\Sigma^2}\right)(\hat{b}_1^\dagger\hat{b}_1 + \hat{b}_1\hat{b}_1^\dagger) + \hbar\frac{\omega_2}{4}\left(1 + \frac{C_2(C_1+C_g)}{C_\Sigma^2}\right)(\hat{b}_2^\dagger\hat{b}_2 + \hat{b}_2\hat{b}_2^\dagger) \\ + \hbar\frac{C_g\sqrt{\omega_1\omega_2 C_1 C_2}}{2C_\Sigma^2}(\hat{b}_1^\dagger\hat{b}_2 + \hat{b}_1\hat{b}_2^\dagger) \\ = \left(1 + \frac{C_1(C_2+C_g)}{C_\Sigma^2}\right)\frac{\hat{\phi}_1^2}{4L_1} + \left(1 + \frac{C_2(C_1+C_g)}{C_\Sigma^2}\right)\frac{\hat{\phi}_2^2}{4L_2} + \frac{\hat{q}_1^2}{4C_1} + \frac{\hat{q}_2^2}{4C_2} + \frac{C_g}{2C_\Sigma^2}\sqrt{\frac{C_1C_2}{L_1L_2}}\hat{\phi}_1\hat{\phi}_2 \\ + \frac{C_g}{4C_\Sigma^2}(\hat{q}_1 + \hat{q}_2)^2\end{aligned} \tag{3.32}$$

The RWA apparently replaces half of the charge coupling with a coupling in flux. The only way to factorize this coupling is $\left(\sqrt{\frac{C_1}{L_1}}\hat{\phi}_1 + \sqrt{\frac{C_2}{L_2}}\hat{\phi}_2\right)^2$ which has no clear circuit

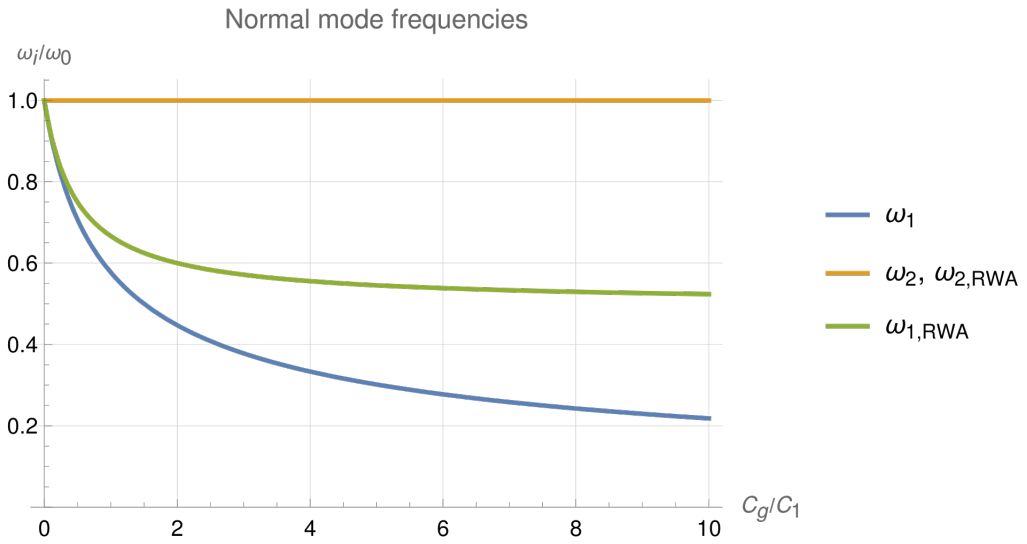

Figure 3.3.2: Normal mode frequencies of the coupled resonator system in units of $\omega_0 \equiv \frac{1}{\sqrt{L_1 C_1}}$ plotted against C_g for exact and RWA Hamiltonian with resonators of equal parameters $C_1 = C_2$ and $L_1 = L_2$.

correspondence. Letting the coupling instead be written as it is in (3.4), the new term can be interpreted as representing a mutual inductance between the resonator circuits. As mutual inductance do not fit within the framework of method of nodes [42], one should be wary of indiscriminate application of RWA as one may end up with the Hamiltonian of an ill-defined circuit. Before moving on, it is prudent to know the difference the RWA has made in the normal modes of the system.

The normal modes may be found in a straightforward manner using (3.26). The RWA Hamiltonian can be written in matrix form as

$$\hat{H}_{RWA} = \frac{1}{2}\boldsymbol{q}^T \begin{bmatrix} \frac{1}{2C_1} + \frac{C_2+C_g}{2C_\Sigma^2} & \frac{C_g}{2C_\Sigma^2} \\ \frac{C_g}{2C_\Sigma^2} & \frac{1}{2C_2} + \frac{C_1+C_g}{2C_\Sigma^2} \end{bmatrix} \boldsymbol{q} + \frac{1}{2}\boldsymbol{\phi}^T \begin{bmatrix} \frac{1}{2L_1} + \frac{C_1(C_2+C_g)}{2C_\Sigma^2 L_1} & \frac{C_g}{2C_\Sigma^2}\sqrt{\frac{L_1 L_2}{C_1 C_2}} \\ \frac{C_g}{2C_\Sigma^2}\sqrt{\frac{L_1 L_2}{C_1 C_2}} & \frac{1}{2L_2} + \frac{C_2(C_1+C_g)}{2C_\Sigma^2 L_2} \end{bmatrix} \boldsymbol{\phi} \tag{3.33}$$

The eigenvalues of $\boldsymbol{C}^{-1}\boldsymbol{L}^{-1}$ and $\boldsymbol{C}_{\mathrm{RWA}}^{-1}\boldsymbol{L}_{\mathrm{RWA}}^{-1}$ in units of $1/\sqrt{C_1 L_1}$ can be seen plotted on Fig. 3.3.3 and 3.3.2 as a function of the capacitive coupling C_g for $L_2 = L_1$ and $L_2 = 4L_1$, respectively. Note how the eigenvalues of the RWA converge with the exact Hamiltonian when $C_g \to 0$, as the anomalous terms vanish when the bosonic modes are uncoupled. As the coupling capacitance increases, however, the normal mode frequencies of the exact and RWA Hamiltonian begin to diverge from each other. For resonators of equal parameters, the first normal mode remain equal to the isolated resonance frequency of both circuits for all coupling strengths. This normal mode corresponds to the eigenvector $\begin{pmatrix} 1 & 1 \end{pmatrix}^T$ and denotes both oscillators moving in phase with one another.

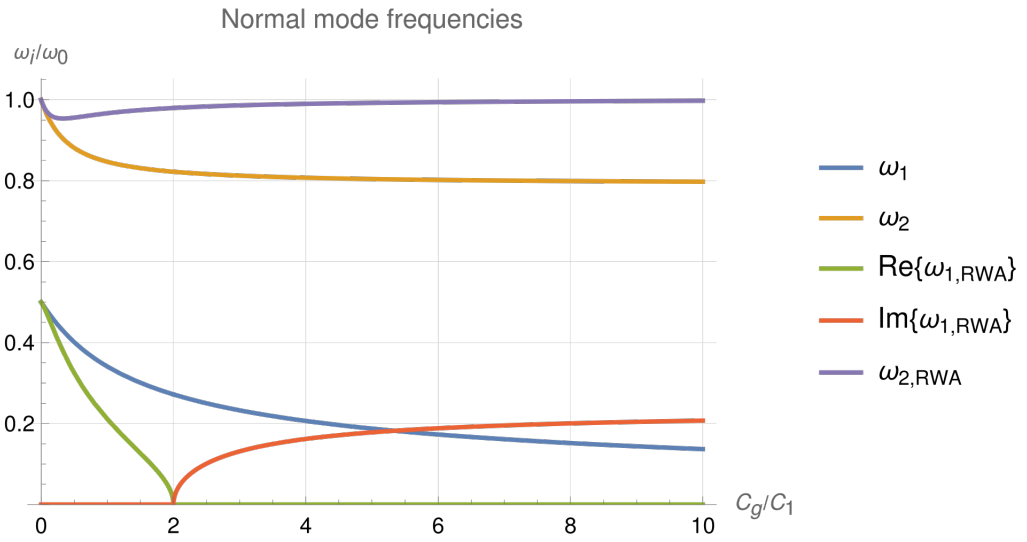

Figure 3.3.3: Normal mode frequencies of the coupled resonator system in units of $\omega_0 \equiv \frac{1}{\sqrt{L_1 C_1}}$ plotted against C_g for exact and RWA Hamiltonian. With $C_2 = C_1$ and $L_2 = 4L_1$.

Since they follow the motion of each other exactly, no interactions between the resonators occur in this mode. The "spring" between them never gets stretched or squeezed. As interactions between boson modes are the source of anomalous terms, only particle conserving processes remain in this normal mode. This is why ω_2 and $\omega_{2,\mathrm{RWA}}$ follow each other exactly on Fig. 3.3.2 as a constant value no matter the magnitude of C_g.

The in-phase normal mode does not exist for resonators of different resonant frequencies however. As seen on Fig. 3.3.3, both RWA normal modes diverge from their exact counterpart with increasing C_g. For a sufficiently large capacitance, the lower frequency RWA normal mode will decrease to zero and then obtain an imaginary value as C_g increases further. In the boson number basis this becomes an imaginary contribution to the system energy with the addition of low frequency normal mode bosons, while in the charge-flux basis the system has obtained a dampening for a system of purely reactive components. Both are non-physical and reveals that the RWA Hamiltonian has become defective with the addition of the mutual inductance term. This suggests that one may only work with an RWA Hamiltonian if the coupling capacitance is small compared to the capacitance of the resonators.

The continuous transmission line

When the physical dimensions of a circuit reach a considerable fraction of its electrical wavelength, the phase and magnitude of current and voltage will vary along the length of its wires [34]. This behavior can be included in circuit analysis by considering the

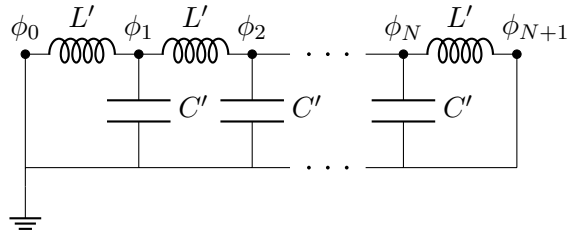

Figure 3.3.4: Circuit diagram of the lossless transmission line as N coupled resonators.

diagram of a coaxial cable seen on Fig. 3.3.4. Coaxial cables consist of an inner conducting cable surrounded by a concentric grounded conductor isolated from each other by a sheet of dielectric material place in between them. The flow of current creates a magnetic field surrounding the wire, resulting in some inductance per unit length, σ_L. The circuit model implements this by having N inductors of inductance L' connected in series along the length of the wire. In addition to flux, the voltage difference between inner and outer wire results in a capacitive charge difference between inner and outer wire per unit length σ_C. This is represented as a series of capacitors of capacitance C' connecting the inductors of the inner wire with the grounded outer conductor [42]. For normal metals, a resistance will also be present along the length of the cable, in addition to a leakage resistance due to imperfections in the dielectric insulator. However, these will be neglected for the purposes of this thesis. By defining a *lattice spacing* Δz, the inductance and capacitance of the transmission line can be written as $C' \equiv \sigma_C \Delta z$ and $L' \equiv \sigma_L \Delta z$. By short-circuiting both ends of the transmission line like in Fig. 3.3.4, the node flux at each endpoint is set to zero $\phi_0 = \phi_{N+1} = 0$. This prevents the inclusion of a zero mode in the normal modes of the transmission line system. Zero modes are normal modes with a frequency of zero. For circuits, they represent a translational freedom of the system, which has no impact on its dynamics. Zero modes can prove troublesome, particularly when performing a Bogoliubov transformation of a second quantized Hamiltonian [10]. Short-circuiting the transmission line endpoints is a simple way of excluding zero modes while keeping the dynamics the same.

With the circuit diagram established and justified, the method of nodes can be applied to obtain the circuit Lagrangian

$$\mathcal{L} = \sum_{n=0}^{N} \left[\frac{\dot{\phi}_n^2}{2} C' - \frac{(\phi_{n+1} - \phi_n)^2}{2L'} \right] \equiv \sum_{n=0}^{N} \left[\frac{\dot{\phi}_n^2}{2} \sigma_C \Delta z - \frac{1}{2\sigma_L} \left(\frac{(\phi_{n+1} - \phi_n)^2}{\Delta z} \right)^2 \Delta z \right] \tag{3.34}$$

Taking the limit $N \to \infty$ together with $\Delta z \to 0$ to keep transmission line length constant

results in the Lagrangian for a continuous transmission line [42]

$$\mathcal{L} = \int_0^l \left[\frac{1}{2}\sigma_C \dot{\phi}^2 - \frac{1}{2\sigma_L}\left(\frac{\partial \phi}{\partial z}\right)^2 \right]^2 dz \tag{3.35}$$

With l being the length of the transmission line and $\phi(t, z)$ now a function allowing temporal and spatial variations in flux. As is known from analytical mechanics, the path of the system in phase space is the one which minimizes its Lagrangian [19]. As node flux is now a continuous function of time t and length z, the Euler-Lagrange equation must also include a z derivative term to minimize the Lagrangian

$$\frac{\partial \mathcal{L}}{\partial \phi} - \frac{d}{dt}\frac{\partial \mathcal{L}}{\partial \dot{\phi}} - \frac{d}{dz}\frac{\partial \mathcal{L}}{\partial \partial_z \phi} = 0 \tag{3.36}$$

As ϕ does not appear in the Lagrangian, only the t and z terms remain in the Euler-Lagrange equation

$$\begin{aligned} \frac{\partial \mathcal{L}}{\partial \dot{\phi}} &= \sigma_C \dot{\phi} \\ \frac{\partial \mathcal{L}}{\partial \partial_z \phi} &= -\frac{1}{\sigma_L}\frac{\partial \phi}{\partial z} \end{aligned} \tag{3.37}$$

With this, the Euler-Lagrange equation takes the form of a wave equation

$$\frac{\partial^2 \phi}{\partial t^2} = \frac{1}{\sigma_C \sigma_L}\frac{\partial^2 \phi}{\partial z^2} \equiv c^2 \frac{\partial^2 \phi}{\partial z^2} \tag{3.38}$$

With $c \equiv 1/\sqrt{\sigma_C \sigma_L}$ being the wave velocity of signals traveling through the transmission line. The normal modes of the transmission line can be found by making the ansatz of back and forward traveling waves

$$\phi(t, z) = \phi_0^- e^{-ikz - i\omega t} + \phi_0^+ e^{ikz - i\omega t} \tag{3.39}$$

As both ends of the transmission line are short-circuited, the fixed endpoints $\phi_0 = \phi_{N+1} = 0$ become the boundary conditions $\phi(t, 0) = \phi(t, l) = 0$. The condition $\phi(t, 0) = 0$ fixes the ratio of the back-and forward traveling waves $\phi_0^+ = -\phi_0^- \equiv \phi_0$. This means that a short-circuited endpoint will send any signal back with equal magnitude and opposite sign, once it reaches the end of the transmission line. The solution is now

$$\phi(t, z) = -2i\phi_0 \sin(kz) e^{-i\omega t} \tag{3.40}$$

The second boundary condition $\phi(t, l) = 0$ gives a discretization condition for the wave number k

$$k = \frac{n\pi}{l}, \quad n = 0,\ 1,\ \ldots,\ N \tag{3.41}$$

Which for the continuous limit $N \to \infty$ implies an infinite but evenly spaced set of modes distributed along the length of the transmission line. The wave number restriction yields the normal mode frequencies via Eq.(3.38)

$$\omega_n = \frac{n\pi c}{l} \tag{3.42}$$

Note that this is a linear relation. In the continuous limit the transmission line will have an infinite set of evenly spaced normal mode frequencies, with an increasing inductive or capacitive density yielding a smaller spacing between frequencies. Or in language more often used in condensed matter physics: a higher density of states.

To keep the normal modes real, any imaginary component is absorbed into the normalization factor ϕ_0 along with introducing the normal mode phase θ_n. The normal modes are then

$$\phi(t,z) = \sum_{n=1}^{\infty} A_n \sin\left(\frac{n\pi}{l}z\right)\cos\left(\frac{n\pi c}{l}t + \theta_n\right) \tag{3.43}$$

As the Lagrangian is an integral across z, it will be convenient to express the diagonalized node fluxes Φ_n as excluding the spatial dependence

$$\Phi_n(t) \equiv A_n \cos(\omega_n t + \theta_n) \tag{3.44}$$

Such that

$$\phi(t,z) = \sum_{n=1}^{\infty} \Phi_n(t)\sin\left(\frac{n\pi c}{l}n\right) \tag{3.45}$$

Substituting the above expression for normal modes into the Lagrangian in (3.35) now yields a sum of integrals

$$\begin{aligned}\mathcal{L} &= \sum_{n=1}^{\infty}\int_0^l \left(\frac{1}{2}\sigma_C\dot{\Phi}_n^2\sin^2\left(\frac{n\pi}{l}z\right) - \frac{\Phi_n^2}{2\sigma_L}\left(\frac{n\pi}{l}\right)^2\cos^2\left(\frac{n\pi}{l}z\right)\right) \\ &= \sum_{n=1}^{\infty}\int_0^{n\pi}\left(\frac{1}{2}\sigma_C\dot{\Phi}_n^2\sin^2(\alpha) - \frac{\Phi_n^2}{2\sigma_L}\left(\frac{n\pi}{l}\right)^2\cos^2(\alpha)\right)\frac{l}{n\pi}d\alpha\end{aligned} \tag{3.46}$$

By performing the change of variable $\alpha \equiv n\pi z/l$, the integral across z can be performed using the following [42]

$$\int_0^{n\pi} d\alpha\cos^2(\alpha) = \int_0^{n\pi} d\alpha\sin^2(\alpha) = \frac{n\pi}{2} \tag{3.47}$$

Making the diagonalized Lagrangian

$$\mathcal{L} = \sum_{n=1}^{\infty}\left(\frac{\sigma_C l}{4}\dot{\Phi}_n^2 - \frac{(n\pi)^2}{4\sigma_L l}\Phi_n^2\right) \equiv \sum_{n=1}^{\infty}\left(\frac{1}{2}C_n\dot{\Phi}_n^2 - \frac{1}{2L_n}\Phi_n^2\right) \tag{3.48}$$

Where $C_n \equiv \sigma_C l/2$ and $L_n \equiv 2\sigma_L l/(n\pi)^2$ are the capacitance and inductance of the transmission line in its diagonalized basis. Note how capacitance remains constant, while the inductance scales with normal modes as $L_n \propto n^{-2}$. The diagonalized node charge can now be found as the conjugate variable of Φ_n

$$Q_n = \frac{\partial \mathcal{L}}{\partial \dot{\Phi}_n} = C_n \dot{\Phi}_n \tag{3.49}$$

Using the above to perform a Legendre transformation yields the Hamiltonian of a continuous transmission line in its diagonal basis

$$\mathcal{H} = \sum_{n=1}^{\infty} \left(\frac{Q_n^2}{2C_n} + \frac{\Phi_n^2}{2L_n} \right) \tag{3.50}$$

The energy of a transmission is thus equal to the energy of an infinite set of non-interacting harmonic oscillators. Since they are all decoupled, a quantum Hamiltonian of a continuous transmission line in second quantization is obtainable in the same manner as the single oscillator quantization presented in section 3.1

$$\hat{H} = \sum_{n=1}^{\infty} \hbar \omega_n \hat{b}_n^\dagger \hat{b}_n \tag{3.51}$$

With ω_n defined in (3.42). An infinite sum might seem to make the Hamiltonian intractable to work with, but as will be seen in section 3.4, it is usually only bosons of some resonant frequency which will be excited.

Discrete transmission line

Before moving on to implementing dissipation in quantum systems, it will be instructive to know the dispersion relation of a transmission line which is kept discrete. Consider again the Lagrangian in (3.34). Keeping $C' = C$ and $L' = L$ as a capacitance and inductance without expressing them in terms of length densities, the Hamiltonian in its original basis can be found through a Legendre transformation

$$\mathcal{H} = \sum_{n=0}^{N} \left[\frac{q_n^2}{2C} + \frac{(\phi_{n+1} - \phi_n)^2}{2L} \right] \tag{3.52}$$

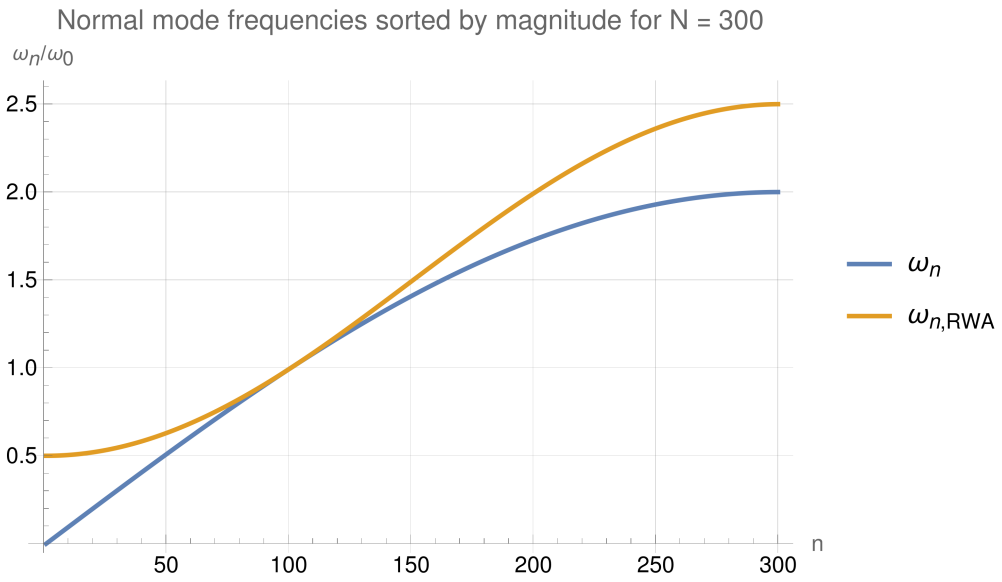

Figure 3.3.5: Exact and RWA dispersion relation for a discrete transmission line with $N = 300$.

Quantizing flux and charge, and then inserting the bosonic operators for each node as defined in (3.4), the Hamiltonian obtains a quadratic form in second quantization

$$\hat{H}/\hbar = \frac{\omega_0}{2}\boldsymbol{b}^\dagger \left[\begin{array}{cccc|cccc} \frac{3}{2} & -\frac{1}{2} & & & \frac{1}{2} & -\frac{1}{2} & & \\ -\frac{1}{2} & \frac{3}{2} & \ddots & & -\frac{1}{2} & \frac{1}{2} & \ddots & \\ & \ddots & \ddots & -\frac{1}{2} & & \ddots & \ddots & -\frac{1}{2} \\ & & -\frac{1}{2} & \frac{3}{2} & & & -\frac{1}{2} & \frac{1}{2} \\ \hline \frac{1}{2} & -\frac{1}{2} & & & \frac{3}{2} & -\frac{1}{2} & & \\ -\frac{1}{2} & \frac{1}{2} & \ddots & & -\frac{1}{2} & \frac{3}{2} & \ddots & \\ & \ddots & \ddots & -\frac{1}{2} & \frac{1}{2} & \ddots & \ddots & -\frac{1}{2} \\ & & -\frac{1}{2} & \frac{1}{2} & & & -\frac{1}{2} & \frac{3}{2} \end{array}\right] \boldsymbol{b} \tag{3.53}$$

With $\boldsymbol{b} \equiv (\,\hat{b}_1 \ldots \hat{b}_N\ \hat{b}_1^\dagger \ldots \hat{b}_N^\dagger\,)^T$ being a vector containing both annihilation and creation operators for each boson mode. The Hamiltonian consists of four tridiagonal blocks, with the particle-conserving terms in the upper left and lower right blocks, and the anomalous terms in the remaining two. Note that the entire basis choice of including both annihilation and creation operators in the same vector is needed to accommodate the anomalous terms. The RWA Hamiltonian is found by neglecting the upper right and lower left blocks

$$\hat{H}_{\mathrm{RWA}}/\hbar = \frac{\omega_0}{2}\boldsymbol{b}^\dagger \begin{bmatrix} \frac{3}{2} & -\frac{1}{2} & & & & & & \\ -\frac{1}{2} & \frac{3}{2} & \ddots & & & & & \\ & \ddots & \ddots & -\frac{1}{2} & & & & \\ & & -\frac{1}{2} & \frac{3}{2} & & & & \\ & & & & \frac{3}{2} & -\frac{1}{2} & & \\ & & & & -\frac{1}{2} & \frac{3}{2} & \ddots & \\ & & & & & \ddots & \ddots & -\frac{1}{2} \\ & & & & & & -\frac{1}{2} & \frac{3}{2} \end{bmatrix} \boldsymbol{b} \tag{3.54}$$

The dispersion relation of the discrete transmission line can now be found via a diagonalizing Bogoliubov transformation[1]. The result can be seen on figure 3.3.5 in units of $\omega_0 \equiv 1/\sqrt{LC}$ for $N = 300$. Note how the dispersion is linear for low n until it tapers off as it approaches $2\omega_0$. This is the discrete dispersion relation

$$\omega_q = \omega_0\sqrt{2\left[1-\cos\left(q\Delta z\right)\right]}, \quad \Delta z = 1, \quad q = \frac{n\pi}{N} \quad \text{for } N \gg 1 \tag{3.55}$$

which is derived in detail in section 4.2, and mirrors the dispersion relation of phonons in one dimension [3]. Though the zero mode is removed by fixing the endpoints, the lowest normal mode frequency approaches zero as the system approaches a continuum $N \to \infty$. Which is why the dispersion for ω_n on Fig. 3.3.5 appears gapless. A wave of vanishing frequency implies that the wave has a diverging wavelength. Such waves will shift each point in the system equally at zero energy expense, which is the source of the translational freedom in the transmission line waveguide. This freedom forces the transmission line to break a continuous translational symmetry in flux. As an equal displacement in flux for the whole system results in a state with the same energy, the current state must necessarily be arbitrarily picked from an infinite set of energetically identical configurations. This is why the Bogoliubov transformation fails for systems with a zero mode. Transformation matrices and their inverses need to be able to go from one basis and back. But for a non-interacting basis that is infinitely degenerate in the number of zero mode bosons, the information of the number of zero mode bosons is lost when going from the non-interacting basis to the interacting one. In the language of linear algebra, the determinant of a transformation denotes the proportion between a volume in the old and new basis. For singular matrices of zero determinant, the dimensionality of a transformed volume has been reduced to a lower number, and no transformation can increase the dimensionality through only a combination of its spanning vectors. In other words, information has been lost which can not be recovered, and transformations to and from the non-interacting basis through linear transformation is impossible.

[1] See appendix C.

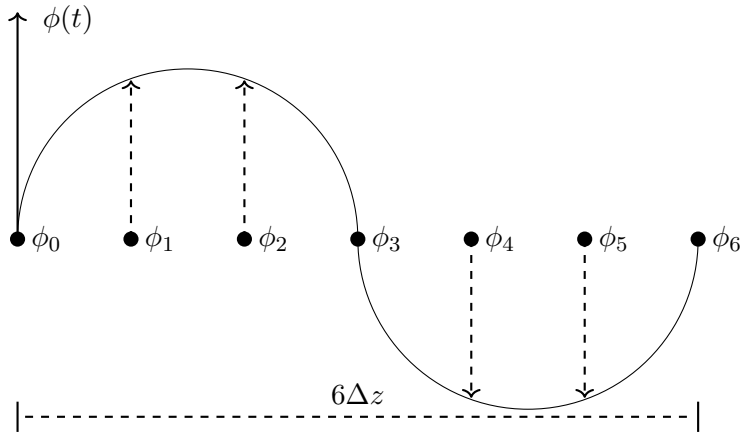

Figure 3.3.6: The standing wave pattern of the waveguide resonant normal mode.

Notably, the RWA has introduced a gap in the dispersion of the system. A gapped dispersion implies that the wave quanta are massive. This is described by the Klein-Gordon equation, which can also model classical systems such as suspended cables and rope bridges [20]. For the discrete RWA transmission line, the dispersion relation can be derived by assuming wave solutions for the dynamical matrix of the system[2]

$$\omega_{\mathrm{RWA}}(\omega) = \frac{1}{2\sqrt{LC}}\sqrt{11 + 2\cos 2q - 12\cos q} \tag{3.56}$$

By setting $q = 0$, the mass of the RWA quanta is seen to be $\omega_0/2$. The presence of two cosines is the result of the dynamical matrix (3.26) for the RWA system containing *next-nearest* neighbor interactions. A dispersion relation of this form is reminiscent of that for the discrete Klein-Gordon equation of a 2D lattice in [12]. This implies that coupling bosonic modes in such a way that anomalous terms always vanish requires more complex geometry than is supported in one dimension.

Note that the RWA becomes exact around the resonant frequency $\omega_n \sim \omega_0$. The reason behind this can be found by considering the wavelength of the normal mode with resonant frequency. Solving the dispersion (3.55) for $\omega_n = \omega_0$ gives the resonant normal mode as $n = N/3$. The corresponding wavelength for this normal mode is then

$$\lambda = \frac{2\pi}{q} = \frac{2N\Delta z}{n} = 6\Delta z \tag{3.57}$$

The wavelength of the resonant normal mode therefore spans exactly six of the resonator cells seen on the circuit diagram in Figure 3.3.4. With the endpoints fixed, the wavelength implies every third node is also fixed at zero flux. The result is a series

[2]See appendix D.

of non-interacting pairs of resonators moving in phase with each other in a standing wave pattern as depicted in Figure 3.3.6. Like the coupling-independent normal mode of the capacitive-coupled resonators in figure 3.3.2, the in-phase movement prevents any difference in flux between non-fixed neighboring nodes. There are then no boson mode interactions and thus all anomalous processes vanish. This is the physical reason why RWA works for systems excited at resonant frequency.

3.4 Reservoirs and Poincaré Recurrences

The inability of Hamiltonian mechanics to include the loss of system energy can be circumvented by including an energy "reservoir" for the system to exchange energy with. Since dissipative equations of motion like Stoke's drag and Ohm's law are linear relations, similar terms can be derived from a reservoir consisting of harmonic oscillators. This leaves the question of how many oscillators an environment should be made up of, and what their parameters should be. Furthermore, the working procedure of quantum mechanics is to split the universe into two parts, the system of interest and the rest of the universe [15]. To include the dissipation of energy from system to "the rest of the universe" in quantum mechanics implies having to solve the Schrödinger equation for the entire universe, an impossible task. Therefore, to include the environment in a literal sense demands some truncation of its size. An instructive example of solving a quantum system coupled to a finite environment is an excited quantum resonator decaying and releasing its energy into N harmonic oscillators [32]. Using the boson particle number basis derived in Sec. 3.1, one is still left with an infinite Hilbert space due to bosons allowing multiple occupations of the same state. To allow a solution of a finite amount of state amplitudes, the Hilbert space is truncated to $N+1$ states by restricting the dynamics to a one particle problem. This implies that all terms of the Hamiltonian must be *particle conserving* to ensure that only a single particle exists at any point in time. Destroying the particle in the resonator therefore requires creating another in one of the reservoir modes. Such a Hamiltonian has the form

$$\hat{H} = \hbar\Omega\hat{a}^\dagger\hat{a} + \sum_{i=1}^{N}\hbar\omega_i\hat{b}_i^\dagger\hat{b}_i + \sum_{i=1}^{N}\gamma_i(\hat{a}\hat{b}_i^\dagger + \hat{a}^\dagger\hat{b}_i) \tag{3.58}$$

With $\hat{a}^{(\dagger)}$ and $\hat{b}_i^{(\dagger)}$ being the annihilation (creation) operators for the resonator and bath mode i respectively as defined by Eq. (3.4), Ω and ω_i the resonant frequencies and γ_i the coupling between system and mode i[3].The Hilbert space is now spanned by the following set of $N+1$ state vectors $\{|0\rangle = |100\ldots0\rangle,\ |1\rangle \equiv |010\ldots0\rangle,\ |i\rangle \equiv |000\ldots1^{(ith),\ldots,0}\}$ corresponding to either the system or reservoir mode i having a single boson excitation.

This Hamiltonian has been used to model the measurement of single photons emitted from qubit decay [33]. The justification of regarding a qubit as a harmonic oscillator lies in the temperature scales of the experiment. Temperatures are of the scale $T \sim 0.01$ K in nanocalorimetry experiments, while the temperature scale for thermal excitation of a superconducting qubit is usually $\hbar\Omega/k_B \sim 0.3\ldots1$ K. This makes two-level state transitions of a qubit functionally equivalent to a harmonic oscillator having one or zero excitations. As for the reservoir modes, any low energy mode which has a non-negligible probability of being excited at 0.01 K will also have its coupling to the qubit scaled with a factor of $\sim(\gamma_i/\hbar\Omega)^2$. Since $\gamma_i/\hbar\Omega$ is usually less than 10^{-4}, the low energy modes can be regarded as isolated. By assuming the modes of the system are in their ground state as a result, exciting the qubit with a π pulse allows an exact solution of the Schrödinger equation for the excitation moving around the system-bath ensemble. Note that the accuracy of the resulting dynamics hinge on the temperature of the experiment being around absolute zero. If temperatures are large enough to allow thermal excitations, it becomes unlikely that only a single boson is moving around at any given time. Not only does this break the $N+1$ states Hilbert space assumption, the qubit can no longer be modelled as an excited resonator due to the possibility of multiple particle occupations. With this in mind, the Schrödinger equation can be solved in the interaction picture by splitting the Hamiltonian into its static non-interaction and time-dependent interaction components [38]

$$\hat{H}_0 \equiv \hbar\Omega\hat{a}^\dagger\hat{a} + \sum_{i=1}^{N}\hbar\omega_i\hat{b}_i^\dagger\hat{b}_i, \quad \hat{V}_I \equiv \sum_{i=1}^{N}\gamma_i\left(\hat{a}^\dagger\hat{b}_i e^{i(\Omega-\omega_i)t} + \hat{a}\hat{b}_i^\dagger e^{-i(\Omega-\omega_i)t}\right) \tag{3.59}$$

The state of the system-bath configuration at time t is given by the superposition of

[3]This often referred to as a *star configuration* with each bath mode only coupled to the system. Another common type of system-bath coupling is the *chain configuration* with the system coupling to the first bath mode, which is coupled to the second mode and so on. The Hamiltonian of a chain configuration can be transformed to that of a star configuration by diagonalizing the bath modes. Likewise, a star configuration can be made into a chain by bringing the Hamiltonian to a tridiagonal form. The chain-to-star diagonalization of bath modes is used in this thesis in chapter 4 for calculating the dissipative properties of a transmission line. The reader interested in star-to-chain tridiagonalization is referred to the following paper on the numerical renormalization group for quantum impurities [4].

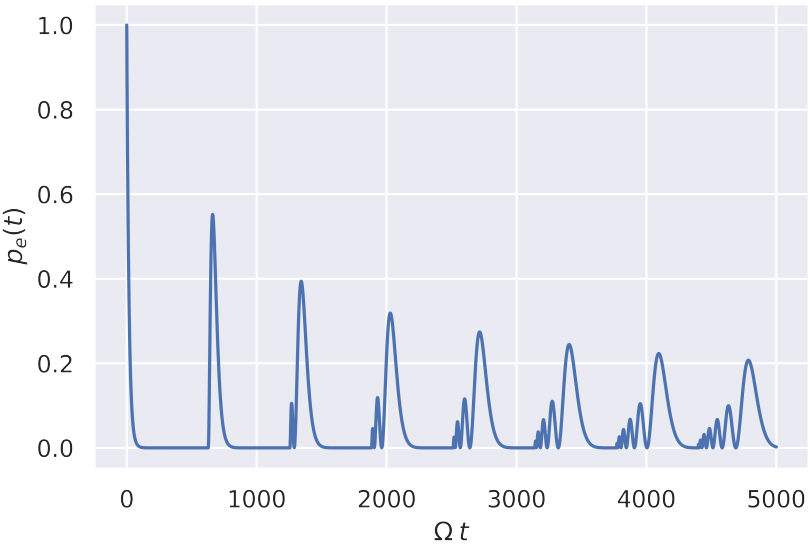

Figure 3.4.1: Probability of qubit excitation at dimensionless normalized time Ωt.

each possible occupation state $|i\rangle$ multiplied with its time dependent state amplitude $\mathcal{C}_i$

$$|\Psi(t)\rangle = \sum_{i=0}^{N} \mathcal{C}_i(t)|i\rangle \tag{3.60}$$

The time evolution of each state amplitude can now be found through the interaction picture Schrödinger equation

$$i\hbar \sum_{i=0}^{N} \dot{\mathcal{C}}(t)|i\rangle = \sum_{j=1}^{N} \left(\hat{a}^\dagger \hat{b}_j e^{i(\Omega-\omega_j)t} + \hat{a}\hat{b}_j^\dagger e^{-i(\Omega-\omega_j)t}\right) \sum_{i=1}^{N} \mathcal{C}_i(t)|i\rangle \tag{3.61}$$

The time evolution $\dot{\mathcal{C}}_0(t)$ of the qubit is found by applying the $\langle 0|$ bra

$$i\hbar\dot{\mathcal{C}}_0(t) = \sum_{i=1}^{N} \gamma_i e^{i(\Omega-\omega_i)t}\mathcal{C}_i(t) \tag{3.62}$$

Likewise, applying $\langle i \neq 0|$ yields the time derivative of each bath mode $\dot{\mathcal{C}}_i(t)$

$$i\hbar\dot{C}_i(t) = \gamma_i e^{-i(\Omega-\omega_i)t} \tag{3.63}$$

Having the qubit excite at $t = 0$ implies the initial condition $|\Psi(0)\rangle = |0\rangle$ which corresponds to $\mathcal{C}_0(0) = 1$ and $\mathcal{C}_i(0) = 0$. The last step before solving Eqs. (3.62) and (3.63) numerically, is choosing a reasonable range of bath frequencies ω_i and their

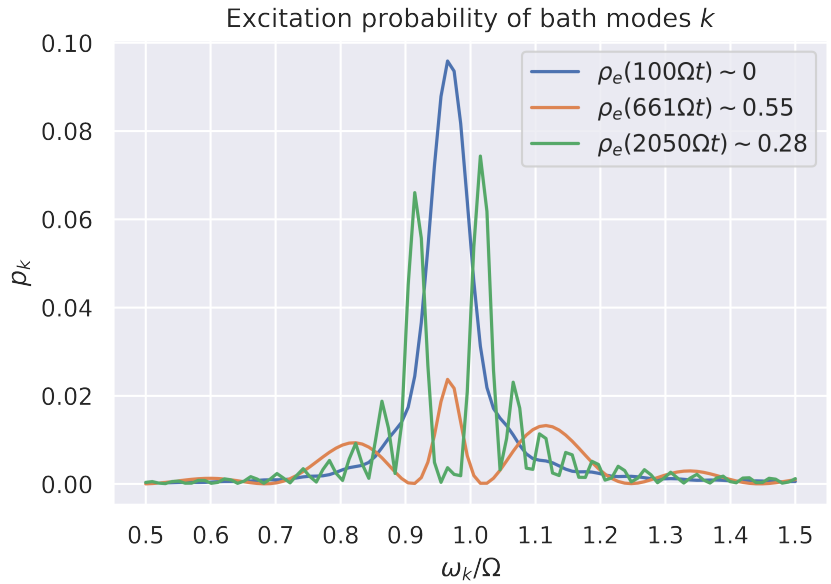

Figure 3.4.2: Excitation probabilities of a subset of bath modes around the qubit frequency at the time instants $100\Omega t$, $661\Omega t$ and $2050\Omega t$, roughly corresponding to the first qubit decay and the first and third recurrences respectively.

coupling to the system γ_i. Motivated by the linear dispersion relation (3.42) for a continuous transmission line, the frequencies are assumed to follow the relation $\omega_k = k\Delta\omega$, with $\Delta\omega$ being the frequency spacing determined from the transmission line's length and wave velocity. In [32] they use the frequency spacing $\Delta\omega = 0.01\Omega$ and $N = 300$ to emulate the waveguide used in the experiment of [47]. By also assuming the "standard coupling" of $\gamma_k = g\sqrt{k}$, the probability of an excited qubit $p_e(t)$ can be found via the Born rule as the squared magnitude of $\mathcal{C}_0(t)$. The resulting probability of an excited qubit can be seen on figure 3.4.1 as a function of normalized time Ωt. It can be seen that the qubit excitation probability decays sharply to 0 before experiencing an almost periodic recovery at around $t = 2\pi/\Delta\omega$. This return to a previous state in phase space is often called a *Poincaré recurrence*. In the analogy of the reservoir as a transmission line, the first recurrence at $t = 2\pi/\Delta\omega$ can be interpreted as the time needed for a signal to travel through the line and be reflected back again to its origin. Increasing the transmission line length will per (3.42) decrease $\Delta\omega$, if wave velocity is kept constant, and thus increase the recurrence time. The reinjection of energy that happens in a Poincaré is incompatible with dissipation as it appears classically. Discharging a capacitor through an Ohmic resistor will never have the resistor recharge the capacitor to its original voltage. Therefore a system, as described by the Hamiltonian

in Eq. (3.58), can only be described as dissipative at timescales below $2\pi/\Delta\omega$. For the frequency spacing given in [32] and the typical superconducting qubit frequency of ~ 5 Ghz [23], this will be around a few picoseconds. Additionally, the excitation probability of bath modes with comparable frequency to Ω is plotted on figure 3.4.2 at three time instants. It is immediately clear that the system couples the strongest to bath modes of similar frequency. This supports the assumption that thermally excited low-frequency bath modes can be regarded as isolated from the system.

As increasing the transmission line length increases the recurrence time, it seems obvious that Poincaré recurrences can be entirely avoided if the length of the transmission line is infinite. This is the idea behind having a reservoir with infinite degrees of freedom, which was proposed by Caldeira and Leggett in their model for quantum dissipation [5]. Direct implementation of this idea makes an exact solution of the Schrödinger equation for the system and bath ensemble impossible, however, and alternative ways of solving for the dynamics of the quantum system must be found. In the following section, it will be shown how infinite degrees of freedom can still lead to tractable equations of motion for a quantum operator in the Heisenberg picture in a so-called reduced system description.

Chapter 4

Heisenberg-Langevin Equation

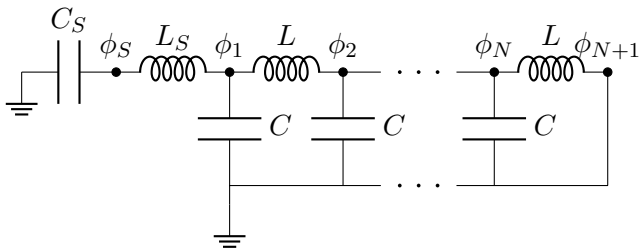

Figure 4.0.1: An LC resonator with capacitance C_S and inductance L_S connected to a lossless transmission line with N modes of effective capacitance C and inductance L.

Phenomenological equations of motion allow the inclusion of dissipation in the description of classical systems. Stoke's drag and Ohm's law being two such examples. As shown in Sec. 1, the inclusion dissipation also implies a reverse process of energy flow into the system from thermal fluctuations in the environment. The dynamics of this can be captured in a Langevin equation containing a velocity dependent friction and random noise term. From this, the statistical properties such as the variance in position and velocity can be calculated for a classical Brownian particle.

A similar description of Brownian motion in a quantum mechanical system is not this simple, however. As the equations of motion for a quantum system is derived from Hamiltonian formalism, any energy expelled from the system must be explicitly included in its Hamiltonian. This can be done by assuming a linear coupling between system and environment. From this, a tractable description of a dissipative quantum system is possible, by modelling the environment as an infinite set of harmonic oscillators. This is known as the independent oscillator model [13, 16]. As will be shown in this section, adopting the Heisenberg picture for such a Hamiltonian results in the environment de-

grees of freedom adding a velocity dependent dissipation term and a stochastic form term to the system's equation of motion.

Consider an LC resonator coupled to a transmission line with N modes as depicted on Fig. 4.0.1. The node ϕ_{N-1} is included and grounded to avoid the zero mode for the reasons mentioned in Sec. 3.3. Using the method of nodes, the following Hamiltonian is obtained

$$H = \frac{q_S^2}{2C_S} + \frac{(\phi_S - \phi_1)^2}{2L_S} + \frac{1}{2C}\sum_{n=1}^{N} q_n^2 + \frac{1}{2L}\sum_{n=1}^{N}(\phi_n - \phi_{n+1})^2 \tag{4.1}$$

For the purposes of the following calculations, it is convenient to express the corresponding quantized Hamiltonian in matrix form

$$\hat{H} \equiv \hat{H}_S + \hat{H}_B + \hat{H}_I$$

$$\hat{H}_S = \frac{\hat{q}_S^2}{2C_S} + \frac{\hat{\phi}_S^2}{2L_S}, \quad \hat{H}_B = \frac{1}{2C}\boldsymbol{q}^T\boldsymbol{q} + \frac{1}{2}\boldsymbol{\phi}^T\boldsymbol{L}_B^{-1}\boldsymbol{\phi}, \quad \hat{H}_I = -\hat{\phi}_S\boldsymbol{V}\boldsymbol{\phi} \tag{4.2}$$

With

$$\boldsymbol{q} \equiv \begin{pmatrix} \hat{q}_1 \\ \hat{q}_2 \\ \vdots \\ \hat{q}_N \end{pmatrix}, \ \boldsymbol{\phi} \equiv \begin{pmatrix} \hat{\phi}_1 \\ \hat{\phi}_2 \\ \vdots \\ \hat{\phi}_N \end{pmatrix}, \ \boldsymbol{L}_B^{-1} \equiv \begin{bmatrix} \frac{1}{L} + \frac{1}{L_S} & -\frac{1}{L} & \\ -\frac{1}{L} & \frac{2}{L} & \ddots \\ & \ddots & \ddots \end{bmatrix}, \ \boldsymbol{V} \equiv \begin{bmatrix} \frac{1}{L_S} & 0 & \dots & 0 \end{bmatrix} \tag{4.3}$$

The time evolution of the system in terms of the node flux operators can be expressed in the Heisenberg picture as[1]

$$C_S\ddot{\hat{\phi}}_S(t) = -\frac{\hat{\phi}_S(t)}{L_S} + \boldsymbol{V}\boldsymbol{\phi}(t), \quad C\ddot{\boldsymbol{\phi}}(t) = -\boldsymbol{L}_B^{-1}\boldsymbol{\phi}(t) + \boldsymbol{V}^T\hat{\phi}_S(t) \tag{4.4}$$

As it is only the system itself which is of interest, it is desirable to "integrate out" the environment degrees of freedom and arrive at a reduced system description. This is done by solving the environment equations of motion and inserting them into the equation for $\ddot{\hat{\phi}}_S$. The linear inhomogeneous ODE's that govern $\boldsymbol{\phi}$ can be solved using the standard method of adding a particular solution to the general solution of the corresponding homogeneous problem. The first step to this, is performing a change of basis to the bath normal modes[2]

$$\ddot{\boldsymbol{\phi}}(t) = -\boldsymbol{U}\boldsymbol{U}^T C^{-1}\boldsymbol{L}_B^{-1}\boldsymbol{U}\boldsymbol{U}^T\boldsymbol{\phi}(t) + C^{-1}\boldsymbol{V}^T\hat{\phi}_S(t) = -\boldsymbol{U}\boldsymbol{\Omega}_B^2\boldsymbol{U}^T\boldsymbol{\phi}(t) + C^{-1}\boldsymbol{V}^T\hat{\phi}_S(t)$$

[1]Note that due the system-bath ensemble consisting only of harmonic oscillators, the following calculations also hold for a classical analysis using Hamilton's equation.

[2]A chain-to-star transformation can be freely performed in the flux-charge basis without breaking canonical commutation relations. As long as the diagonalizing transformation applied to $\boldsymbol{\phi}$ is also applied to $\boldsymbol{q}$, commutation relations will be preserved.

$$\downarrow$$

$$\ddot{\boldsymbol{\Phi}}(t) = -\boldsymbol{\Omega}_{\boldsymbol{B}}^2 \boldsymbol{\Phi}(t) + \frac{1}{\sqrt{C}} \boldsymbol{U}^T \boldsymbol{V}^T \hat{\phi}_S(t) \tag{4.5}$$

With $\boldsymbol{U}$ being the unitary matrix of right eigenvectors that diagonalize $C^{-1}\boldsymbol{L}_B^{-1}$, $\boldsymbol{\Omega}_B^2$ the corresponding diagonal matrix of eigenvalues and $\boldsymbol{\Phi} \equiv \sqrt{C}\boldsymbol{U}^T\boldsymbol{\phi}$ the normal mode basis. By scaling the normal modes with $\sqrt{C}$, the similar transformation $\boldsymbol{Q} \equiv 1/\sqrt{C}\boldsymbol{U}\boldsymbol{q}$ can be made, such that the normal mode basis of the bath Hamiltonian is expressed purely in terms of frequency whilst preserving canonical commutation relations.

The homogeneous problem is now

$$\ddot{\boldsymbol{\Phi}}(t) = -\boldsymbol{\Omega}_B^2 \boldsymbol{\Phi}(t) \tag{4.6}$$

Which can be solved with the ansatz

$$\boldsymbol{\Phi}(t) = \cos[\boldsymbol{\Omega}_B(t - t_0)]\boldsymbol{a} + \sin[\boldsymbol{\Omega}_B(t - t_0)]\boldsymbol{b} \tag{4.7}$$

The vector coefficients $\boldsymbol{a}$ and $\boldsymbol{b}$ are determined by the initial conditions

$$\boldsymbol{\Phi}(t_0) = \boldsymbol{a}$$

$$\dot{\boldsymbol{\Phi}}(t_0) = \boldsymbol{Q}(t_0) = \boldsymbol{\Omega_B}\boldsymbol{b} \tag{4.8}$$

Making the general solution for the homogeneous problem in the normal mode basis

$$\boldsymbol{\Phi}(t) = \cos[\boldsymbol{\Omega}_B(t - t_0)]\boldsymbol{\Phi}(t_0) + \frac{\sin[\boldsymbol{\Omega}_B(t - t_0)]}{\boldsymbol{\Omega}_B}\dot{\boldsymbol{\Phi}}(t_0) \tag{4.9}$$

As the Heisenberg and Schrödinger picture coincide at $t = t_0$, $\boldsymbol{\Phi}(t_0)$ is to be interpreted as a vector of time independent Schrödinger operators for the bath's degrees of freedom.

A particular solution to the inhomogeneous problem can be found via the Green's function method [2]. Think of $\boldsymbol{\Phi}(t)$ as a collection of particles being acted upon by $\boldsymbol{f}(t) \equiv 1/\sqrt{C}\boldsymbol{U}^T\boldsymbol{V}^T\hat{\phi}_S(t)$ as a time dependent force. This force manifests as a series of momentary impulses starting at time t_0[3]. The state of these particles at a later time t can then be found by integrating the product of this force with a Green's function representing the particles' response to it. The particular solution therefore has the form

$$\boldsymbol{\Phi}_p(t) = \int_{t_0}^{\infty} dt' \boldsymbol{G}(t, t')\boldsymbol{f}(t') \tag{4.10}$$

With $\boldsymbol{G}(t, t')$ being a matrix Green's function following the causal boundary conditions $\boldsymbol{G}(t_0, t') = \dot{\boldsymbol{G}}(t_0, t') = \boldsymbol{0}$. Writing $\boldsymbol{f}(t') = \int_{t_0}^{\infty} \boldsymbol{f}(t')\delta(t - t')$, Eq. (4.5) becomes

$$\int_{t_0}^{\infty} dt' \left(\ddot{\boldsymbol{G}}(t, t') + \boldsymbol{\Omega}_B^2 \boldsymbol{G}(t, t')\right) \boldsymbol{f}(t') = \int_{t_0}^{\infty} dt' \boldsymbol{f}(t')\delta(t - t') \tag{4.11}$$

[3]Think of the collision between water molecules and a pollen particle in prototypical Brownian motion.

Removing the integral and $\boldsymbol{f}(t')$ from both sides imposes the following relation on $G(t,t')$

$$\ddot{\boldsymbol{G}}(t,t') + \boldsymbol{\Omega}_B^2 \boldsymbol{G}(t,t') = \hat{I}\delta(t-t') \tag{4.12}$$

Fourier transforming the above yields the bath's response in frequency space for the normal mode basis

$$\boldsymbol{G}(\omega) = \frac{1}{\boldsymbol{\Omega}_{\boldsymbol{B}}^2 - \hat{I}(\omega^2 + i\eta)^2} \tag{4.13}$$

Eq. (4.12) can be solved by performing a Laplace transformation and applying the causal boundary conditions

$$\int_0^\infty dt \ddot{\boldsymbol{G}}(t,t')e^{-pt} + \boldsymbol{\Omega}_B^2 \int_0^\infty dt \boldsymbol{G}(t,t')e^{-pt} = (p^2\hat{I} + \boldsymbol{\Omega}_B^2)\int_0^\infty dt \boldsymbol{G}(t,t') = e^{-pt'}\hat{I}$$

$$\downarrow$$

$$\int_0^\infty dt \boldsymbol{G}(t,t') = \frac{e^{-pt'}}{p^2\hat{I} + \boldsymbol{\Omega}_B^2} \tag{4.14}$$

The inverse Laplace transform gives the real time Green's function [2]

$$\boldsymbol{G}(t,t') = \frac{\sin[\boldsymbol{\Omega}_B(t-t')]}{\boldsymbol{\Omega}_B}\Theta(t-t') \tag{4.15}$$

Making the particular solution

$$\boldsymbol{\Phi}_p(t) = \frac{1}{\sqrt{C}}\int_{t_0}^t \frac{\sin[\boldsymbol{\Omega}_B(t-t')]}{\boldsymbol{\Omega}_B}\boldsymbol{U}^T\boldsymbol{V}^T\hat{\phi}_S(t) \tag{4.16}$$

And the complete solution of $\boldsymbol{\Phi}(t)$

$$\boldsymbol{\Phi}(t) = \cos[\boldsymbol{\Omega}_B(t-t_0)]\boldsymbol{\Phi}(t_0) + \frac{\sin[\boldsymbol{\Omega}_B(t-t_0)]}{\boldsymbol{\Omega}_B}\dot{\boldsymbol{\Phi}}(t_0) + \sqrt{C}\int_{t_0}^t \frac{\sin[\boldsymbol{\Omega}_B(t-t')]}{\boldsymbol{\Omega}_B}\boldsymbol{U}^T\boldsymbol{V}^T\hat{\phi}_S(t) \tag{4.17}$$

Which in the original basis is

$$\boldsymbol{\phi}(t) = \boldsymbol{U}\cos[\boldsymbol{\Omega}_B(t-t_0)]\boldsymbol{U}^T\boldsymbol{\phi}(t_0) + \boldsymbol{U}\frac{\sin[\boldsymbol{\Omega}_B(t-t_0)]}{\boldsymbol{\Omega}_B}\boldsymbol{U}^T\dot{\boldsymbol{\phi}}(t_0) + \frac{1}{C}\int_{t_0}^t dt'\boldsymbol{U}\frac{\sin[\boldsymbol{\Omega}_B(t-t')]}{\boldsymbol{\Omega}_B}\boldsymbol{U}^T\boldsymbol{V}^T\hat{\phi}_S(t) \tag{4.18}$$

Note that imposing causal boundary conditions on the inhomogeneous equation has resulted in a retarded Green's function. Using this solution therefore breaks time-reversal symmetry, as is desired for any description of a dissipative system [16].

Inserting this into the original expression for $\ddot{\hat{\phi}}_S$ completes the integration of the bath degrees of freedom and a description containing only the system of interest is obtained.

$$C_S\ddot{\hat{\phi}}_S(t) = -\frac{\hat{\phi}_S(t)}{L_S} + \hat{\eta}(t) + \int_{t_0}^t dt'\Sigma(t-t')\hat{\phi}_S(t) \tag{4.19}$$

With

$$\hat{\eta}(t) \equiv \boldsymbol{V}\boldsymbol{U}\cos[\boldsymbol{\Omega}_B(t-t_0)]\boldsymbol{U}^T\boldsymbol{\phi}(t_0) + \boldsymbol{V}\boldsymbol{U}\frac{\sin[\boldsymbol{\Omega}_B(t-t_0)]}{\boldsymbol{\Omega}_B}\boldsymbol{U}^T\dot{\boldsymbol{\phi}}(t_0),$$

$$\Sigma(t-t') \equiv \frac{1}{C}\boldsymbol{V}\boldsymbol{U}\frac{\sin[\boldsymbol{\Omega}_B(t-t')]}{\boldsymbol{\Omega}_B}\boldsymbol{U}^T\boldsymbol{V}^T \tag{4.20}$$

By assuming the bath is in thermal equilibrium, $\boldsymbol{\phi}(t_0)$ and $\dot{\boldsymbol{\phi}}(t_0)$ can be distributed according to the Boltzmann distribution. This, along with the infinite degrees of freedom, causes $\hat{\eta}(t)$ to act as a *stochastic noise operator*. While the scalar value $\Sigma(t-t')$ is deterministic, it causes the integral in which it resides to become *non-local* in time. It is therefore referred to as *memory kernel*. All influence the bath exerts on the system is encoded within these two terms. It should now be stated that the thermodynamic limit $N \to \infty$ of the bath is taken to prevent Poincaré recurrences[4] [46].

While the system now has a stochastic term in its equation of motion, it does not yet have velocity dependent damping. This can be introduced by defining the *dissipation kernel* [13]

$$\gamma(t-t') \equiv \frac{1}{C}\boldsymbol{V}\boldsymbol{U}\frac{\cos[\boldsymbol{\Omega}_B(t-t')]}{\boldsymbol{\Omega}_B^2}\boldsymbol{U}^T\boldsymbol{V}^T \tag{4.21}$$

Making it the negative derivative of the memory kernel: $\Sigma(t) = -\dot{\gamma}(t)$. Inserting this and performing partial integration results in

$$C_S\ddot{\hat{\phi}}_S(t) = -\frac{\hat{\phi}_S(t)}{L_S} + \left[\gamma(t-t')\hat{\phi}_S(t')\right]_{t_0}^{t} - \int_{t_0}^{t} dt'\gamma(t-t')\dot{\hat{\phi}}_S(t) + \hat{\eta}(t) \tag{4.22}$$

The boundary term at $t' = t$ is

$$\gamma(0)\hat{\phi}_S(t) = \frac{1}{C}\boldsymbol{V}\boldsymbol{U}\frac{1}{\boldsymbol{\Omega}_B^2}\boldsymbol{U}^T\boldsymbol{V}^T\hat{\phi}_S(t) = \frac{1}{C}\boldsymbol{V}(\boldsymbol{U}^T\boldsymbol{\Omega}_B^2\boldsymbol{U})^{-1}\boldsymbol{V}^T\hat{\phi}_S(t) = \boldsymbol{V}\boldsymbol{L}_B\boldsymbol{V}^T\hat{\phi}_S(t)$$

$$= \frac{1}{L_S^2}[\boldsymbol{L}_B]_{11}\hat{\phi}_S(t) = \frac{1}{L_S^2}\left(\frac{N}{\frac{1}{L}+\frac{N}{L_S}}\right)\hat{\phi}_S(t) = \frac{\hat{\phi}_S(t)}{L_S} \tag{4.23}$$

Where the thermodynamic limit $N \to \infty$ is used in the last step.

For mathematical purposes the limit $t_0 \to -\infty$ is taken to allow the use of the Fourier transform and simplifying expressions such as the boundary term at $t' = t_0$

$$\lim_{t_0 \to -\infty} \gamma(t-t')\hat{\phi}_S(t') = \gamma(\infty)\hat{\phi}_S(-\infty) = 0 \tag{4.24}$$

The dissipation kernel vanishing at ∞ will be shown in the analytical calculation of the memory kernel. Inserting the boundary terms, the expression for $\ddot{\phi}_S(t)$ finally obtains the familiar form

$$C_S\ddot{\hat{\phi}}_S(t) = -\int_{-\infty}^{t} dt'\gamma(t-t')\dot{\hat{\phi}}_S(t') + \hat{\eta}(t) \tag{4.25}$$

[4]This limit will also be used for simplifying expressions such as Eq.(4.23)

Which is known as the *Heisenberg-Langevin equation* of a free particle, which can be used to compute statistical properties in the same manner as the classical Langevin equation. This is an alternative approach to density operators in the study of open quantum systems, with the distinct property of including of memory effects [41]. Before moving on to the computation of statistical properties, some important concepts and terminology in the study of open quantum systems must first be introduced.

4.1 Spectral distributions and characterizing reservoirs

Know that the damping term in the Heisenberg-Langevin equation can be rewritten as a *convolution*

$$-\int_{-\infty}^{t} dt\gamma(t-t')\dot{\hat{\phi}}_S(t') = -\int_{-\infty}^{\infty} dt\gamma(t-t')\dot{\hat{\phi}}_S(t')\Theta(t-t') \equiv -(\gamma^+ * \dot{\hat{\phi}}_S)(t) \tag{4.26}$$

Where $\gamma^+(t) \equiv \gamma(t)\Theta(t)$ is the *right sided* damping kernel. This is useful as the *convolution theorem* [2] can be applied when performing the Fourier transform of Eq. (4.25)

$$-C_S\omega^2\hat{\phi}_S(\omega) = i\omega\gamma^+(\omega)\hat{\phi}_S(\omega) + \hat{\eta}(\omega) \tag{4.27}$$

And similarly for the Fourier transformation of Eq.(4.19)

$$-C_S\omega^2\hat{\phi}_S(\omega) = \left(\Sigma^+(\omega) - \frac{1}{L_S}\right)\hat{\phi}(\omega) + \hat{\eta}(\omega) \tag{4.28}$$

From which it can be deduced

$$i\omega\gamma^+(\omega) = \Sigma^+(\omega) - \frac{1}{L_S} \tag{4.29}$$

Solving (4.27) for $\hat{\psi}_S(\omega)$ gives the response function of the system to the stochastic fluctuations from $\hat{\eta}(\omega)$

$$G^+(\omega) \equiv \frac{1}{-i\omega\gamma^+(\omega) - C_S(\omega+i\eta)^2} = \frac{1}{\frac{1}{L_S} - C_S(\omega+i\eta)^2 - \Sigma^+(\omega)} \tag{4.30}$$

From this it can be inferred that it is in fact the right sided functions $\gamma^+(\omega)$ and $\Sigma^+(\omega)$, which characterizes the system's coupling to the bath. As the imaginary component of the response functions denotes dampening, it is specifically Re $\gamma^+(\omega)$ and Im $\Sigma^+(\omega)$ which describes the dissipation of energy from the system into the reservoir. For this reason, Re $\gamma^+(\omega)$ is referred to as the *spectral distribution*, while the closely related yet distinct quantity Im $\Sigma^+(\omega)$ is known as the *bath spectral density*[5] [22]. It it worthwhile

[5] In the literature it is commonly written as $J(\omega)$.

to know that $\gamma^+(\omega)$ has three important mathematical properties which can be derived from physical principles [16]. The first of these is causality: the system only responds to past forces. This implies that $\gamma^+(z)$ is an analytical function in the upper half of the complex plane for the complex variable z. As a consequence, the *Kramers-Kronig* relates the real and imaginary part of $\gamma^+(\omega)$[30]

$$\mathrm{Re}\,\gamma^+(\omega) = \mathcal{P}\int_{-\infty}^{\infty}\frac{dz}{\pi}\frac{\mathrm{Im}\,\gamma^+(z)}{z-\omega}, \quad z \in \mathbb{C} \tag{4.31}$$

The second property is the *reality condition*

$$\gamma(\omega + i\eta) = \gamma(-\omega + i\eta)^* \tag{4.32}$$

A consequence of $\hat{\phi}_S(t)$ being a Hermitian operator.

The third property follows from the second law of thermodynamics

$$\mathrm{Re}\,\gamma(\omega + i\eta) \leq 0, \quad \infty < \omega < \infty \tag{4.33}$$

Which can be proven by considering an arbitrary force $f(t)$ acting on the system. It is assumed that $f(t)$ vanishes at $t = \pm\infty$. The thermodynamic work can then be found by integrating the product of this force with mean velocity

$$W = \int_{-\infty}^{\infty} dt f(t)\langle\dot{\phi}(t)\rangle \geq 0 \tag{4.34}$$

Invoking Parseval's formula, the work in Fourier space becomes

$$W = \frac{1}{2\pi}\int_{-\infty}^{\infty} d\omega \tilde{f}(\omega)\langle\dot{\tilde{\phi}}(-\omega)\rangle \geq 0 \tag{4.35}$$

Now consider $f(t)$ acting on Eq.(4.25). Taking the mean and performing the Fourier transform yields

$$\tilde{f}(\omega) = [-iC\omega + \tilde{\gamma}(\omega + i\epsilon)]\langle\dot{\tilde{\phi}}(\omega)\rangle \tag{4.36}$$

The work is now

$$W = \frac{1}{2\pi}\int_{-\infty}^{\infty} d\omega[-iC\omega + \tilde{\gamma}(\omega + i\epsilon)]\langle\dot{\tilde{\phi}}(\omega)\rangle\langle\dot{\tilde{\phi}}(-\omega)\rangle \geq 0 \tag{4.37}$$

Invoking the reality condition (4.32 simplifies the integral to

$$W = \frac{1}{\pi}\int_{0}^{\infty} d\omega \mathrm{Re}\{\tilde{\gamma}(\omega + i\epsilon)\}|\langle\dot{\phi}(\omega)\rangle|^2 \geq 0 \tag{4.38}$$

Since the mean system velocity $\langle\dot{\phi}\rangle$ is made arbitrary through $f(t)$, the only way to ensure the above holds is by the condition $\mathrm{Re}\{\tilde{\gamma}(\omega + i\epsilon)\} \geq 0$.

Spectral density classifications

In the phenomenological modelling of quantum dissipation, the bath spectral density written as $J(\omega)$ is commonly assumed to be a smooth function of ω following a power law $J(\omega) \propto \omega^s$ at small frequencies [6, 22, 46]. Here the exponent s characterizes the dissipative properties of the bath, of which there are three qualitatively different cases. Before delving into the properties of these, it should be noted that the spectral distribution is related to the spectral density by[6]

$$\operatorname{Re}\gamma^+(\omega) = \frac{\operatorname{Im}\Sigma^+(\omega)}{\omega} \tag{4.39}$$

For $s = 1$ the spectral density has a linear dependence on ω and is known as an *Ohmic bath*. An Ohmic bath implies a real and frequency independent spectral distribution per Eq. (4.39), making the time dependence of the dissipation kernel a delta function. The damping term in Eq.(4.25) then becomes local in time and the dissipation is Markovian as a result. Do note that this does not imply that the bath is memoryless, as noise can still be correlated in time.

Spectral densities with $s < 1$ are referred to as "supraohmic" and densities with $0 < s < 1$ are known as "subohmic". Both of these two bath types appear much less frequently in the litterature than their Ohmic counterpart [40].

4.2 An analytical expression of the memory kernel

Consider the right sided Fourier transform of the memory kernel in (4.20)

$$\mathcal{F}\{\Sigma(t)\Theta(t)\} = \Sigma^+(\omega) = \frac{1}{C}\boldsymbol{V}\boldsymbol{U}\frac{1}{\boldsymbol{\Omega}_{\boldsymbol{B}}^2 - (\omega+i\eta)^2\hat{I}}\boldsymbol{U}^T\boldsymbol{V}^T \tag{4.40}$$

By finding an analytical expression for the eigenvectors and eigenvalues of $C^{-1}\boldsymbol{L}_B^{-1}$, the memory kernel can be expressed exact. However, this is very complicated due to the presence of L_S as a kind of "impurity" in $\boldsymbol{L}_B^{-1}$. Fortunately, the homogeneous case with $L = L_S$ can be diagonalized in a straightforward manner, and the general solution for $\Sigma^+(\omega)$ can be deduced from the definition of the reservoir's Green's function [14]. Notice that the right-sided memory kernel is the diagonalized response function of the bath $\boldsymbol{g}^+(\omega)$[7] multiplied by the system-bath coupling squared

$$\Sigma^+(\omega) = \boldsymbol{V}\boldsymbol{g}^+(\omega)\boldsymbol{V}^T = \boldsymbol{V}\frac{1}{\boldsymbol{L}_B^{-1} - C(\omega+i\eta)^2\hat{I}}\boldsymbol{V}^T = \frac{1}{C}\frac{1}{L_S^2}\left[\boldsymbol{U}\frac{1}{\boldsymbol{\Omega}_{\boldsymbol{B}}^2 - (\omega+i\eta)^2\hat{I}}\boldsymbol{U}^T\right]_{11} \tag{4.41}$$

[6] Seen by taking the imaginary part of (4.29).

[7] Found by Fourier transforming the right equation in (4.4) and taking the reciprocal prefactor of $\boldsymbol{V}^T\hat{\psi}_S$ resulting from solving for $\boldsymbol{\phi}(\omega)$.

By defining the homogeneous matrix $\boldsymbol{L}_{B,0}^{-1}$ as $\boldsymbol{L}_B^{-1}$ with $L_S = L$ and the perturbation matrix $\Delta\boldsymbol{L}^{-1}$ with $\left[\Delta\boldsymbol{L}^{-1}\right]_{11} = 1/L_S - 1/L$ being its only non-zero element, the bath response function can be written as

$$\boldsymbol{g}^+(\omega) = \frac{1}{\boldsymbol{L}_{B,0}^{-1} + \Delta\boldsymbol{L}^{-1} - (\omega + i\eta)^2\hat{I}}$$

$$\downarrow$$

$$\boldsymbol{g}^+(\omega)\left[\boldsymbol{g}_0^{+-1} + \Delta\boldsymbol{L}^{-1}\right] = \hat{I}$$

$$\downarrow$$

$$\boldsymbol{g}^+(\omega) = \frac{\boldsymbol{g}_0^+(\omega)}{\hat{I} + \Delta\boldsymbol{L}^{-1}\boldsymbol{g}_0^+(\omega)} \tag{4.42}$$

Where $\boldsymbol{g}_0^+ \equiv \left[\boldsymbol{L}_{B,0}^{-1} - (\omega + i\eta)^2\hat{I}\right]$ is the homogeneous bath response function.

With this result it is only necessary to find the eigenvectors and eigenvalues of $C^{-1}\boldsymbol{L}_{B,0}^{-1}$. The eigenvalue problem can be written as

$$\frac{1}{CL}\boldsymbol{F}\boldsymbol{\Psi}^q = \lambda^q\boldsymbol{\Psi}^q \tag{4.43}$$

With $\boldsymbol{\Psi}^q$ being the eigenvectors, λ^q the eigenvalues and $\boldsymbol{F}$ the tridiagonal matrix

$$\boldsymbol{F} \equiv \begin{bmatrix} 2 & -1 & \\ -1 & 2 & \ddots \\ & \ddots & \ddots \end{bmatrix} \tag{4.44}$$

There are thus only three unique equations for this matrix problem

$$F_{11}\Psi_1^q + F_{12}\Psi_2^q = \lambda^q\Psi_1^q$$

$$F_{NN}\Psi_N^q + F_{NN-1}\Psi_{N-1}^q = \lambda^q\Psi_N^q$$

$$F_{mm}\Psi_m^q + F_{mm-1}\Psi_{m-1}^q + F_{mm+1}\Psi_{m+1}^q = \lambda^q\Psi_m^q, \quad m = 2,\, 3,\, \ldots,\, N-1 \tag{4.45}$$

The first two constitute the boundary equations, while the third is the "bulk" equation. Such a system of equations is reminiscent of the string problem, and it is therefore prudent to look for solutions in the form of forward and backward propagating waves

$$\Psi_m^q = e^{iqm} + Be^{-iqm} \tag{4.46}$$

As the eigenvectors can be normalized at a later point, only the ratio B between the waves is written currently. Inserting this ansatz into the bulk equation gives the relation

$$(\lambda^q - 2)\left(e^{iqm} + Be^{-iqm}\right) = -\left(e^{iq(m+1)} + Be^{-iq(m+1)} + e^{iq(m-1)} + Be^{-iq(m-1)}\right)$$

$$= -\left(e^{iq} + Be^{-iq}\right)\left(e^{iq} + e^{-iq}\right) = -2\cos q\left(e^{iqm} + Be^{-iqm}\right) \tag{4.47}$$

The eigenvalues must therefore be[8]

$$\lambda^q \equiv \omega_q^2 = \frac{2}{LC}(1 - \cos q) \tag{4.48}$$

It now remains to determine the wave ration B and restrictions on q from the boundary equations. The equation at $m = 1$ states

$$2\cos q\left(e^{iq} + Be^{-iq}\right) = e^{2iq} + Be^{-2iq} \tag{4.49}$$

Solving for B

$$B = \frac{e^{2iq} - 2e^{iq}\cos q}{2e^{-iq}\cos q - e^{-2iq}} = \frac{e^{iq} - 2\cos q}{2\cos q - e^{-iq}} = -\frac{e^{-iq}}{e^{iq}}e^{2iq} = -1 \tag{4.50}$$

The backward propagating waves are therefore of equal amplitude but perfectly out of phase with those propagating forward. With the wave ration obtained, the last boundary equation can be used to derive a selection criteria for q

$$2\cos q\ \left(e^{iqN} + Be^{-iqN}\right) = e^{iq(N-1)} + Be^{-iq(N-1)} \tag{4.51}$$

Solving for B and inserting (4.50) yields

$$1 = e^{2iq(N+1)} \rightarrow q = \frac{n\pi}{N+1}, \quad n = 1,\ 2,\ \ldots,\ N \tag{4.52}$$

The eigenvector elements are therefore proportional to

$$\Psi_m^q \propto e^{i\frac{\pi qm}{N+1}} - e^{-i\frac{\pi qm}{N+1}} = \frac{1}{2i}\sin\frac{\pi qm}{N+1} \tag{4.53}$$

By demanding the eigenvectors to be real and of norm 1, the normalized eigenvectors of $C^{-1}\boldsymbol{L}_{B,0}^{-1}$ are found to be

$$\boldsymbol{\Psi}^q = \sqrt{\frac{2}{N+1}}\begin{pmatrix} \sin\frac{\pi q}{N+1} \\ \sin\frac{2\pi q}{N+1} \\ \vdots \\ \sin\frac{N\pi q}{N+1} \end{pmatrix} \tag{4.54}$$

Making the diagonalizing matrix $\boldsymbol{U}$

$$\boldsymbol{U} = \sqrt{\frac{2}{N+1}}\begin{bmatrix} \sin\frac{\pi}{N+1} & \sin\frac{2\pi}{N+1} & \ldots & \sin\frac{N\pi}{N+1} \\ \sin\frac{2\pi}{N+1} & \sin\frac{4\pi}{N+1} & \ldots & \sin\frac{2N\pi}{N+1} \\ \vdots & \vdots & \ddots & \vdots \\ \sin\frac{N\pi}{N+1} & \sin\frac{2N\pi}{N+1} & \ldots & \sin\frac{N^2\pi}{N+1} \end{bmatrix} \tag{4.55}$$

[8]Remember the proportionality factor $\frac{1}{LC}$ which relates $\boldsymbol{F}$ and $C^{-1}\boldsymbol{L}_{B,0}^{-1}$.

Which is both unitary and symmetric, making $\boldsymbol{U}$ its own inverse.

The first element of the homogeneous response function $\boldsymbol{g}_0^+$ then given by the sum

$$\left[\boldsymbol{g}_0^+\right]_{11} = \frac{1}{C}\frac{2}{N+1}\sum_{q=1}^{N}\frac{\sin^2\frac{\pi q}{N+1}}{\frac{2}{LC}\left(1-\cos\frac{\pi q}{N+1}\right)-(\omega+i\eta)^2} \tag{4.56}$$

By invoking the thermodynamic limit of $N \to \infty$, the spacing between eigenvalues tend to zero and the sum can be replaced by the integral [3]

$$\left[g_0^+\right]_{11} = \frac{2}{\pi C}\int_0^{\pi}\frac{\sin^2 q}{\frac{2}{LC}(1\cos q)-(\omega+i\eta)^2} \tag{4.57}$$

Using the substitution

$$x \equiv \sin\frac{q}{2}, \quad dx\frac{1}{2}\cos\frac{q}{2} \tag{4.58}$$

The integral becomes[9]

$$\left[\boldsymbol{g}_0^+\right]_{11} = \frac{16L}{\pi}\int_0^1 dx\frac{x^2\sqrt{1-x^2}}{4x^2-\alpha^2-i\epsilon} \tag{4.59}$$

With $\alpha^2 \equiv \frac{\omega^2}{LC} = \frac{\omega^2}{\omega_0^2}$. This can be integrated in the limit $\epsilon \to 0^+$

$$\left[g_0^+\right]_{11} = \frac{L}{2}\left(2+\alpha^2\left[\sqrt{1-\frac{4}{\alpha^2}}-1\right]\right) = \frac{L}{2}\left(2-\alpha^2+\sqrt{\alpha^4-4\alpha^2}\right)$$

$$= L\left(1-\frac{\alpha^2}{2}+\sqrt{\left(1-\frac{\alpha^2}{2}\right)^2-1}\right) = L\left(1-\frac{\omega^2}{2\omega_0^2}+\sqrt{\left(1-\frac{\omega^2}{2\omega_0^2}\right)^2-1}\right) \tag{4.60}$$

Which is a complex number for $|\omega| < 2\omega_0$. Combining this result with (4.41) and (4.42) gives an analytic expression for the right sided memory kernel in Fourier space

$$\Sigma^+(\omega) = \frac{1}{L_S^2}\frac{1-\frac{\omega^2}{2\omega_0^2}+\sqrt{\left(1-\frac{\omega^2}{2\omega_0^2}\right)^2-1}}{\frac{1}{L}+(\frac{1}{L_S}-\frac{1}{L})\left(1-\frac{\omega^2}{2\omega_0^2}+\sqrt{\left(1-\frac{\omega^2}{2\omega_0^2}\right)^2-1}\right)} \tag{4.61}$$

[9]Any coefficients of the imaginary component η has been absorbed into the new quantity ϵ. Such a rewrite is of no consequence as both η and ϵ approach 0^+ at the end of the calculation.

4.3 Obtaining Drude dissipation

Using the eigenvalue relation in (4.48), Eq. (4.61) can be written as[10]

$$\Sigma^+(\omega) = \frac{1}{L_S^2}\frac{e^{-|q''|}\cdot e^{iq'(\omega)}}{\frac{1}{L}+\left(\frac{1}{L_S}-\frac{1}{L}\right)e^{-|q''|}\cdot e^{iq'(\omega)}}, \quad q(\omega) = \arccos\left[1-\frac{\omega^2}{2\omega_0^2}\right] \tag{4.62}$$

As the spectral density is only non-zero when q is real, the imaginary component of the above expression simplifies to

$$\mathrm{Im}\left\{\Sigma^+(\omega)\right\} \equiv J(\omega) = \mathrm{Im}\left\{\frac{1}{L_S^2}\frac{1}{\left|\frac{e^{-iq}}{L}+\frac{1}{L_S}-\frac{1}{L}\right|^2}\right\} = \frac{L}{L_S^2}\frac{\omega\sqrt{CL}\sqrt{1-\frac{\omega^2 LC}{4}}}{\frac{L^2}{L_S^2}+\left(1-\frac{L}{L_S}\right)\omega^2 CL} \tag{4.63}$$

By decomposing the bath capacitance and inductance into the product of their density and lattice spacing, the spectral density becomes

$$J(\omega) = \frac{\omega}{\sigma_L}\sqrt{\frac{\sigma_C}{\sigma_L}}\frac{\omega\sqrt{1-\frac{\omega^2\sigma_L\sigma_C a^2}{4}}}{1+\left(1-\frac{\sigma_L a}{L_S}\right)\omega^2\frac{\sigma_C}{\sigma_L}L_S^2} \tag{4.64}$$

With $\sigma_C \equiv C/\Delta z$ and $\sigma_L \equiv L/\Delta z$ being the capacitive and inductive densities. Taking the limit $\Delta z \to 0$ whilst keeping σ_C and σ_L constant[11] leads to a continuum description with the spectral density taking the form

$$J(\omega) = \frac{\omega\gamma_0}{1+\omega^2\tau^2} \tag{4.65}$$

Wehere $\gamma_0 \equiv \sqrt{\frac{\sigma_C}{\sigma_L}}$ and $\tau \equiv \gamma_0 L_S$.

The Drude dissipation kernel can be derived directly from (4.65) by noting that $\gamma(t)$ is a real number. This allows one to write Eq. (4.39) as

$$\frac{J(\omega)}{\omega} = \mathrm{Re}\left\{\gamma^+(\omega)\right\} = \int_{-\infty}^{\infty} dt'\gamma(t')\Theta(t')\cos(\omega t') \tag{4.66}$$

Performing the inverse Fourier transform gives

$$\int_{-\infty}^{\infty}\frac{d\omega}{2\pi}\frac{J(\omega)}{\omega}e^{-i\omega t} = \int_{-\infty}^{\infty}\frac{d\omega}{2\pi}\int_{-\infty}^{\infty}dt\gamma(t)\Theta(t)\frac{e^{-i\omega(t-t')}+e^{-i\omega(t+t')}}{2}$$

$$= \int_{-\infty}^{\infty}dt\gamma(t)\Theta(t)\frac{\delta(t-t')+\delta(t+t')}{2} = \frac{1}{2}\gamma(t)\Theta(t)+\frac{1}{2}\gamma(-t)\Theta(-t) = \frac{1}{2}\gamma(|t|) \tag{4.67}$$

[10] See appendix B.

[11] This also implies $C \to 0$ and $L \to 0$, though these limits do not appear explicitly in the calculation.

By multiplying with $\Theta(t)$, the awkward absolute value of t can be disregarded. Now solving for $\gamma(t)$ and inserting (4.65)

$$\gamma(t) = \Theta(t)\frac{\gamma_0}{\tau^2}\int_{-\infty}^{\infty}\frac{d\omega}{\pi}\frac{e^{-i\omega t}}{\omega^2+\frac{1}{\tau^2}} = \Theta(t)\frac{\gamma_0}{\tau^2}\int_{-\infty}^{\infty}\frac{d\omega}{\pi}\frac{e^{-i\omega t}}{\left(\omega+\frac{i}{\tau}\right)\left(\omega-\frac{i}{\tau}\right)} \tag{4.68}$$

The above integral can be evaluated using the residue theorem. As Jordan's lemma requires that only the simple pole in the lower complex half-plane be included in the clockwise-oriented contour, the evaluated integral becomes

$$\gamma(t) = \Theta(t)\frac{\gamma_0}{\pi\tau^2}\left(-2i\pi\frac{e^{-t/\tau}}{-2\frac{i}{\tau}}\right) = \Theta(t)\frac{\gamma_0}{\tau}e^{-t/\tau} \tag{4.69}$$

This is known as *Drude dampening* [46] and the dissipation kernel does indeed vanish when $t \to \infty$. With this, Heisenberg-Langevin equation takes the form

$$C_S\ddot{\hat{\phi}}_S(t) = -\frac{\gamma_0}{\tau}\int_{-\infty}^{t}dt' e^{-(t-t')/\tau}\dot{\hat{\phi}}_S(t') + \hat{\eta}(t) \tag{4.70}$$

Before moving on to calculating statistical quantities such as the correlation functions, it should be mentioned that taking the strong coupling limit $1/L_S \to \infty$ causes the memory time scale τ to vanish. The bath becomes Ohmic as a consequence, with associated spectral density and dissipation kernel

$$J_{\text{Ohmic}}(\omega) = \gamma_0\omega, \quad \gamma_{\text{Ohmic}}(t-t') = \gamma_0\delta(t-t') \tag{4.71}$$

Which leads to the dissipation term in the Heisenberg-Langevin equation to become local in time. Note that this does not necessarily imply a bath without memory. As will be shown in the following section, the equilibrium time correlator of $\hat{\eta}(t)$ does not generally follow a Dirac delta time scale. Such a system can therefore be said to have Markovian dissipation and non-Markovian fluctuations.

4.4 Statistical properties of the noise term

At first glance $\hat{\eta}(t)$ appears to be deterministic. Given some distribution of $\mathbf{\Phi}(t_0)$ and $\dot{\mathbf{\Phi}}(t_0)$, the system fluctuations seem to follow exactly from (4.20). However, the thermodynamic limit $N \to \infty$ makes direct computation of $\hat{\eta}(t)$'s influence on the dynamics of the system impossible. Instead this noise term must be considered a stochastic quantity, whose statistical properties such as mean and correlation function can be derived, as was done for the Johnson-Nyquist term in section 2.3. The key difference being that the environment is now known microscopically. The derivation of $\langle\hat{\eta}(t)\rangle$ and $\langle\hat{\eta}(t)\hat{\eta}(t')\rangle$ can

then be directly performed using quantum statistics instead of various assumptions like a white noise power spectrum.

Deriving the mean is trivial in thermal equilibrium. Expressing (4.20) as a sum and changing the basis from flux and charge to non-interacting bosons with the bosonic operators from (3.4)

$$\hat{\eta}(t) = \sum_{n=1}^{N} \left\{ \frac{U_{1n}}{L_S\sqrt{C}} \cos[\Omega_n(t-t_0)]\hat{\Phi}_n(t_0) + \frac{U_{1n}}{L_S\sqrt{C}} \frac{\sin[\Omega_n(t-t_0)]}{\Omega_n} \hat{Q}_n(t_0) \right\}$$

$$= \sqrt{\hbar} \sum_{n=1}^{N} \left\{ \frac{U_{1n}}{L_S\sqrt{2C\Omega_n}} \cos[\Omega_n(t-t_0)](\hat{b}_n^\dagger + \hat{b}_n) + i \frac{U_{1n}\sqrt{\Omega_0 C}}{L_S\sqrt{2C}} \frac{\sin[\Omega_n(t-t_0)]}{\Omega_n} (\hat{b}_n^\dagger - \hat{b}_n) \right\} \tag{4.72}$$

Taking the thermal average of the above expression yields $\langle\hat{\eta}(t)\rangle = 0$, as the thermal average of particle non-conserving terms must vanish [46]. The vanishing mean of the stochastic term is thus no longer an assumption, but follows directly from the behavior of non-interacting bosons in thermal equilibrium.

As the system is harmonic, it now remains to find the correlation function $\langle\hat{\eta}(t)\hat{\eta}(t')\rangle$ to know the behavior of the stochastic term. Writing the thermal average of the product of $\hat{\eta}$ with itself at times t and t'

$$\langle\hat{\eta}(t)\hat{\eta}(t')\rangle = \sum_{n,m=1}^{N} \Big\{ \Lambda_n(t)\Lambda_m(t')\langle\hat{\Phi}_n(t_0)\hat{\Phi}_m(t_0)\rangle + \Lambda_n(t)\Gamma_m(t')\langle\hat{\Phi}_n(t_0)\hat{Q}_m(t_0)\rangle$$

$$+\Gamma_n(t)\Lambda_m(t')\langle\hat{Q}_n(t_0)\hat{\Phi}_m(t_0)\rangle + \Gamma_n(t)\Gamma_m(t')\langle\hat{Q}_n(t_0)\hat{Q}_m(t_0)\rangle \Big\} \tag{4.73}$$

With $\Lambda_n(t) \equiv U_{1n}/(L_S\sqrt{C})\cos[\Omega_n(t-t_0)]$ and $\Gamma(t) \equiv U_{1n}/(L_S\sqrt{C})\sin[\Omega_n(t-t_0)]/\Omega_n$. The thermal averages can now be computed

$$\langle\hat{\Phi}_n(t_0)\hat{\Phi}_m(t_0)\rangle = \frac{\hbar}{2\sqrt{\Omega_n\Omega_m}} \left(\langle\hat{b}_n^\dagger\hat{b}_m\rangle + \langle\hat{b}_n\hat{b}_m^\dagger\rangle \right) \delta_{nm} = \frac{\hbar}{2\Omega_n}(2n_B(\Omega_n)+1)$$

$$\langle\hat{Q}_n(t_0)\hat{Q}_m(t_0)\rangle = \frac{\hbar\sqrt{\Omega_n\Omega_m}}{2} \left(\langle\hat{b}_n^\dagger\hat{b}_m\rangle + \langle\hat{b}_n\hat{b}_m^\dagger\rangle \right) \delta_{nm} = \frac{\hbar\Omega_n}{2}(2n_B(\Omega_n)+1)$$

$$\langle\hat{\Phi}_n(t_0)\hat{Q}_m(t_0)\rangle = -i\frac{\hbar}{2} \left(\langle\hat{b}_n^\dagger\hat{b}_m\rangle - \langle\hat{b}_n\hat{b}_m^\dagger\rangle \right) \delta_{nm} = -\langle\hat{Q}_n(t_0)\hat{\Phi}_n(t_0)\rangle = \frac{i\hbar}{2} \tag{4.74}$$

With $n_B(\omega)$ being the Bose-Einstein distribution function. Now finding products of the time dependent terms

$$\Lambda_n(t)\Lambda_n(t') = \frac{U_{1n}^2}{2L_S^2C} \left(\cos[\Omega_n(t+t'-2t_0)] + \cos[\Omega_n(t-t')] \right)$$

$$\Gamma_n(t)\Gamma_n(t') = \frac{U_{1n}^2}{2L_S^2 C\Omega_n^2}\left(\cos[\Omega_n(t-t')] - \cos[\Omega_n(t+t'-2t_0)]\right)$$

$$\Gamma_n(t)\Lambda_n(t') = \frac{U_{1n}^2}{2L_S^2 C\Omega_n}\left(\sin[\Omega_n(t+t'-2t_0)] + \sin[\Omega_n(t-t')]\right)]$$

$$\Lambda_n(t)\Gamma_n(t') = \frac{U_{1n}^2}{2L_S^2 C\Omega_n}\left(\sin[\Omega_n(t+t'-2t_0)] - \sin[\Omega_n(t-t')]\right) \tag{4.75}$$

The noise correlation can then be written as

$$\begin{aligned}\langle\hat{\eta}(t)\hat{\eta}(t')\rangle &= \sum_{n=1}^{N}\Big\{\Lambda_n(t)\Lambda_n(t')\langle\hat{\Phi}_n\hat{\Phi}_n\rangle + \Gamma_n(t)\Gamma_n(t')\langle\hat{Q}_n\hat{Q}_n\rangle \\ &\quad + \left(\Lambda_n(t)\Gamma_n(t') - \Gamma(t)\Lambda(t')\right)\langle\hat{\Phi}_n\hat{Q}_n\rangle\Big\} \qquad (4.76)\\ &= \sum_{n=1}^{N}\frac{\hbar U_{1n}^2}{L_S^2 C\Omega_n}\Big\{(2n_B(\Omega_n)+1)\cos[\Omega_n(t-t')] - i\sin[\Omega_n(t-t')]\Big\}\end{aligned}$$

Which is not a real number for $t \neq t'$. This is the result of the stochastic term now being an operator which in general does not commute at different times. As a result, the nose correlation as it is written above is not observable. This incongruity with classical physics motivated the definition of the *symmetrized noise correlator* [25, 30] which is a real number that serves as the quantum analogue of the classical noise correlation function

$$\frac{1}{2}\left[\langle\hat{\eta}(t)\hat{\eta}(t')\rangle + \langle\hat{\eta}(t')\hat{\eta}(t)\rangle\right] = \sum_{n=1}^{N}\frac{\hbar U_{1n}^2}{L_S^2 C\Omega_n}\Big\{(2n_B(\Omega_n)+1)\cos[\Omega_n(t-t')]\Big\} \tag{4.77}$$

There are two important limits of this expression. In the high temperature limit the noise does not depend on $\hbar$

$$\frac{1}{2}\langle\{\hat{\eta}(t),\hat{\eta}(t')\}\rangle = \sum_{n=1}^{N}\frac{2U_{1n}^2}{L_S^2 C\Omega_n^2}\cos[\Omega_n(t-t')]k_BT, \quad \hbar\Omega_n \ll k_BT \tag{4.78}$$

meaning that these fluctuations are classical [30]. Unlike the classical noise of (2.35), quantum noise does not vanish at zero temperature

$$\frac{1}{2}\langle\{\hat{\eta}(t),\hat{\eta}(t')\}\rangle = \sum_{n=1}^{N}\frac{\hbar U_{1n}^2}{L_S^2 C\Omega_n}\cos[\Omega_n(t-t')], \quad \hbar\Omega_n \gg k_BT \tag{4.79}$$

these are the so-called *zero-point fluctuations* (ZPF). One could be led to believe that this result serves as a quantum correction for a fluctuating system at low temperature, but it has been pointed out in the literature that ZPF's are not observable by classical detectors,

as ordinary photo detectors do not respond to vacuum fluctuations [17, 27]. That is not to say that the derived low temperature quantum fluctuations are non-physical. They can still be detected indirectly stimulating emission of an excited quantum detector. However this phenomena is a different process than quantum Brownian motion of a particle.

Finally it should be noted that (4.77) contains the dissipation kernel (4.21) in the form of a sum. This makes the high temperature limit behave like Johnson-Nyquist noise. For a continuous transmission line, the noise correlations will therefore have an exponentially decaying memory. The fluctuation-dissipation theorem is thus also seen to hold for quantum systems.

4.5 Finding a classical analogue of the quantum circuit

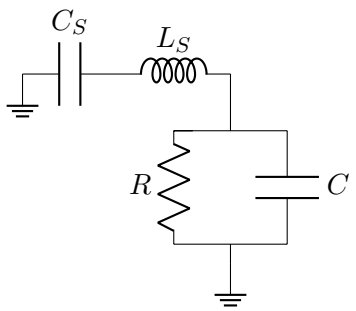

Figure 4.5.1: An LC resonator with capacitance C_S and inductance L_S connected to a parallel RC circuit with resistance R and capacitance C. Serves as the classical analogue to the quantum LC connected to a continuous transmission line bath.

While the infinite transmission line succeeded in providing dissipative dynamics into a quantum system, will remain a mere abstraction if it can not be mapped unto a physically realizable system. It is therefore desirable to find the analogous classical circuit. In the same manner that the spectral density Σ^+ could be related to the response function of the bath $\boldsymbol{g}^+$, the classical counterpart to figure 4.0.1 must be given by a circuit with an impedance that somehow matches the response function of $\hat{\phi}_S$. Consider the response function of (4.30) for Drude dampening with Σ^+ given by (4.65)

$$G^+(\omega) = \frac{1}{\frac{1}{L_S} - C_S\omega^2 - \frac{\omega\gamma_0}{1+\omega^2\tau^2}} \tag{4.80}$$

Finding the classical correspondence now amounts to finding a similar response function, but derived from the application of Ohm's and Kirchhoff's laws to a classical circuit. The

form of G^+ implies that this counterpart can be found in connecting the LC resonator of 4.0.1 to an RC-circuit in parallel as seen on figure 4.5.1. Using the Fourier space version of Ohm's law which was derived in section 2.2, the relation between voltage drop and current through the resonator must be

$$V(\omega) = \frac{1}{\frac{i}{C_S\omega} - iL_S\omega + Z_{RC}(\omega)} I(\omega) \tag{4.81}$$

Where $Z_{RC}(\omega)$ is the impedance of the RC-subcircuit. Examining the RC closer, the RC-impedance is found from (2.20) and (2.18) through the formula for combining impedances in parallel from (2.21)

$$Z_{RC}(\omega) = \frac{1}{\frac{1}{R} - i\omega C} = \frac{R}{1 - i\omega\tau} = \frac{R + i\omega R\tau}{1 + \omega^2\tau^2} \tag{4.82}$$

Where $\tau \equiv CR$. Note that the imaginary component has a similar form to the Drude spectral density

$$\text{Im } Z_{RC}(\omega) = \frac{\omega R\tau}{1 + \omega^2\tau^2} \tag{4.83}$$

Except a difference in units. From 4.65, it can be seen that spectral densities are measured in admittance per time, while impedances are per definition measured in ohm. The correspondence must then be achieved in the response function.

Now writing (4.81) as

$$V(\omega) = \frac{iC_s\omega}{C_S L_S\omega^2 - 1 + iC_S\omega Z_{RC}(\omega)} I(\omega) \tag{4.84}$$

And changing from voltage and current to flux and charge

$$\phi(\omega) = \frac{L_S}{C_S} \frac{i\omega C_S}{C_S L_S\omega^2 - 1 + iC_S\omega Z_{RC}(\omega)} q(\omega) = \frac{1}{-C_S\omega^2 + \frac{1}{L_S} - i\frac{C_S}{L_S}\omega Z_{RC}(\omega)} \dot{q}(\omega) \tag{4.85}$$

Which can be recognized as having the same form as the response function of the quantum circuit (4.80). That the circuit on figure 4.5.1 corresponds to the continuum limit of 4.0.1 can be seen by identifying the imaginary part of the denominator in (4.85) with a Drude spectral density

$$\Sigma^+_{\text{classical}}(\omega) = \frac{C_S}{L_S}\omega \text{Re } Z_{RC}(\omega) = \frac{C_S}{L_S} \frac{R\omega}{1 + \omega^2\tau^2} \tag{4.86}$$

Which has units of admittance per time, as it should. This reveals that the calculations done on the system-bath model of figure 4.0.1 has been a quantum mechanical treatment of the classical dissipative circuit of 4.5.1. With this it has been shown that the lossy dynamics of classical systems can be implemented in quantum mechanics.

Chapter 5

Conclusion

The motivation behind this project was to examine if dissipation could be included in the description of a quantum system, and thereby gain a better understanding of the relationship between a quantum mechanical description and a classical one. For this purpose the formalism of circuit QED as a quantum counterpart to classical circuit theory to allow straightforward comparison between the two physical frameworks. Per the fluctuation-dissipation theorem, stochastic fluctuations were included as a necessary component of dissipative systems, and derived for a classical RLC circuit to serve as the canonical example of classic Brownian motion. Using the method of nodes to design Hamiltonians, the dynamics of various coupled resonator networks were examined. Including an analysis of the RWA of a transmission line, showing that the resonant frequency match with the exact Hamiltonian stems from the corresponding normal mode having no interactions between the dynamic nodes of the feedline. Additionally, the RWA dispersion was shown to be gapped, as a result of RWA creating next-nearest neighbor interactions. With the continuum transmission line as inspiration, the principles of thermal reservoirs were shown with a model of a circuit photon moving through the boson modes of a finite waveguide, with Poincaré recurrences as a necessarry consequence of a finite environment. Finally a reduced-system description of a resonator circuit coupled to an infinite reservoir was implemented in the form of a Heisenberg-Langevin equation showing memory effects in both its dissipation term and in the time correlation of its stochastic noise. In the limit of a continuous transmission line with a smooth density of states, the spectral density of the bath was shown to match that of Drude dissipation, which is the simplest model for dissipation which is regularized for high frequencies. The equilibrium mean an correlation of the stochastic operator was calculated, and it was then shown that quantum noise correlations must be defined with the anti-commutator if they are to be interpreted in the same manner as classical noise. This was due to the noncommutativity of quantum operators leading to an imaginary

component. Furthermore, the Bose-Einstein statistics used in computing the statistical properties of noise lead to a term which is independent of temperature, the zero-point fluctuations, which are unique to quantum systems. The high temperature limit was shown to be independent of $\hbar$, and being of a similar form to the John-Nyquist noise correlation derived for the classical damped resonator. Finally, it was shown that a Heisenberg-Langevin equation with Drude dissipation is the quantum version of an LC resonator coupled to a parallel RC circuit, showing that models of quantum dissipation are physically implementable with classic circuits.

Further work on this topic could involve improving the thermal bath model of [32] by writing the exact Hamiltonian of a cavity coupled to a feedline, and include the anomalous particle terms of the Hamiltonian in a reduced-system description with a Heisenberg-Langevin equation of the particle number operator. This would require a consistent method of obtaining the proper Bogoliubov transformation matrices of a quadratic bosonic Hamiltonian.

Additionally, the circuit QED framework could be utilized to implement more exotic reservoirs. The Rubin model feedline bath serves as a conventional type of reservoir, but so-called *anomalous dissipative couplings* [1, 11], which have properties distinct from the standard dissipation derived in this project, could be implemented with the high amount of freedom circuits allow in the design of quantized Hamiltonians.

Appendix A

Integral transform conventions

Various integral transform are applied throughout this project. As their conventions can vary in the literature, the ones used in this thesis are here explicitly stated to prevent confusion.

The Fourier transform

$$f(t) = \int_{-\infty}^{\infty} \frac{d\omega}{2\pi} f(\omega) e^{-i\omega t}$$
$$f(\omega) = \int_{-\infty}^{\infty} dt f(t) e^{i\omega t} \tag{A.1}$$

The Windowed Fourier transform

$$f_T(\omega) = \frac{1}{\sqrt{T}} \int_{-T/2}^{T/2} f(t) e^{i\omega t} \tag{A.2}$$

Where T is the sampling time of a signal. This definition is required due to the Fourier transform not existing for stationary processes. The power spectrum is defined as the squared magnitude of some stationary process $f(t)$

$$I_f \equiv \lim_{T\to\infty} \frac{1}{T} |f_T(\omega)|^2 \tag{A.3}$$

The Laplace transform

$$F(p) = \int_0^{\infty} dt f(t) e^{-pt} \tag{A.4}$$

Appendix B

Rewriting the homogeneous bath response function

According to [13] the homogeneous bath response function $\left[\boldsymbol{g}^0\right]_{11}$ can be written as

$$\left[\boldsymbol{g}^0(\omega)\right]_{11} \stackrel{?}{=} Le^{iq(\omega)}, \quad q(\omega) = \arccos\left[1 - \frac{\omega^2}{2\omega_0^2}\right] \tag{B.1}$$

However, this rewrite is dubious due to the ambiguity of sign in q's imaginary part. In fact, this substitution causes the real part of the response function to diverge as $\omega \to \infty$. To intuit the correct expression, consider Eq. (4.48)

$$\cos q = 1 - \frac{\omega^2}{2\omega_0^2} \tag{B.2}$$

This can be rewritten as

$$e^{iq} + e^{-iq} = 2\left(1 - \frac{\omega^2}{2\omega_0^2}\right) \tag{B.3}$$

Multiplying with e^{iq} and using the substitution $x \equiv e^{iq}$ leads to the quadratic equation

$$x^2 - 2\left(1 - \frac{\omega^2}{2\omega_0^2}\right)x + 1 = 0 \tag{B.4}$$

With the solution

$$x = 1 - \frac{\omega^2}{2\omega_0^2} \pm i\sqrt{1 - \left(1 - \frac{\omega^2}{2\omega_0^2}\right)^2} = e^{iq} \tag{B.5}$$

This is identical with the numerator in (4.61) *except* for the $\pm$ in front of the imaginary term. This implies that one must take the absolute value of q's imaginary component when substituting Eq. (4.48) into (4.61). The correct form of (B.1) is therefore

$$\left[\boldsymbol{g}^0\right]_{11} = Le^{-|q''|}e^{iq'} \tag{B.6}$$

Which decays to 0 as $\omega \to \infty$. As it should for the inverse Fourier transform to be convergent. In addition, note that $|\omega| > 2\omega_0$ implies $\left(1 - \frac{\omega^2}{2\omega_0^2}\right)^2 > 1$, making the response function an entirely real number. This implies that the spectral density is a vanishing quantity at these frequencies.

Appendix C

The Bogoliubov transformation

One must be careful in the diagonalization of a Hamiltonian with bosonic operators. As a change of basis implies a linear combination of terms in the former basis, diagonalizing a Hamiltonian with anomalous terms will generally mix annihilation and creation operators in such a way that the new basis does not satisfy canonical commutation relations. The resulting bosons will be nonphysical and the dispersion relation inconsistent with one for a basis following canonical commutation rules. Transforming to a diagonal basis with bosons satisfying canonical commutation is called a diagonalizing *Bogoliubov transformation* and will generally be more involved than simply finding the eigenvectors of the Hamiltonian that is to be transformed.

Consider the quadratic bosonic Hamiltonian [8, 43]

$$\hat{H} = \frac{1}{2}\boldsymbol{b}^\dagger \boldsymbol{H} \boldsymbol{b} \tag{C.1}$$

With $\boldsymbol{H}$ being some Hermitian matrix and $\boldsymbol{b} \equiv (\, \hat{b}_1 \, ... \, \hat{b}_N \, \hat{b}_1^\dagger \, ... \, \hat{b}_N^\dagger \,)^T$ a vector containing the creation and annihilation operator of each bosonic mode of the system following canonitcal commutation relations

$$[\hat{b}_i, \hat{b}_j^\dagger] = \hat{b}_i \hat{b}_j^\dagger - \hat{b}_j^\dagger \hat{b}_i = \delta_{ij}, \quad [\hat{b}_i, \hat{b}_j] = \hat{b}_i^\dagger, \hat{b}_j^\dagger] = 0 \tag{C.2}$$

The proper diagonalization of (C.1) requires a homogeneous linear transformation of the N pairs of bosonic operators $\hat{b}_i^{(\dagger)}$ into another set of bosonic operators $\hat{\beta}_i^{(\dagger)}$ which also satisfies (C.2) and brings the Hamiltonian to a diagonal form

$$\hat{H} = \sum_{n=1}^{N} \hbar\omega_n \hat{\beta}_n^\dagger \hat{\beta}_n + \text{constant} \tag{C.3}$$

Or in other words, a set of non-interacting bosons. This greatly simplifies the calculation of a system's time evolution, as well as allowing the application of Bose-Einstein statistics to find analytic expressions for equilibrium correlation functions.

The general expression for the transformation matrices is [43]

$$\mathcal{A} = \begin{bmatrix} \boldsymbol{\mathcal{U}} & \boldsymbol{\mathcal{S}} \\ \boldsymbol{\mathcal{V}} & \boldsymbol{\mathcal{T}} \end{bmatrix}, \quad \mathcal{A}' = \begin{bmatrix} \tilde{\boldsymbol{\mathcal{U}}} & \tilde{\boldsymbol{\mathcal{V}}} \\ \tilde{\boldsymbol{\mathcal{S}}} & \tilde{\boldsymbol{\mathcal{T}}} \end{bmatrix} \tag{C.4}$$

Where each matrix entry is itself an $N \times N$ matrix. From these the new operators are related to the original basis as

$$\boldsymbol{\beta}^\dagger = \boldsymbol{b}^\dagger \mathcal{A}, \quad \boldsymbol{\alpha} = \mathcal{A}' \boldsymbol{b} \tag{C.5}$$

This allows one to write out the diagonalizing transformation explicitly

$$\begin{aligned} \hat{\beta}_m^\dagger &= \sum_{n=1}^{N} \left\{ \hat{b}_n^\dagger \mathcal{U}_{nm} + \hat{b}_n \mathcal{V}_{nm} \right\}, \quad \hat{\beta}_m = \sum_{n=1}^{N} \left\{ \hat{b}_n^\dagger \mathcal{S}_{nm} + \hat{b}_n \mathcal{T}_{nm} \right\} \\ \hat{\alpha}_m &= \sum_{n=1}^{N} \left\{ \tilde{\mathcal{U}}_{mn} \hat{b}_n + \tilde{\mathcal{V}}_{mn} \hat{b}_n^\dagger \right\}, \quad \hat{\alpha}_m^\dagger = \sum_{n=1}^{N} \left\{ \tilde{\mathcal{S}}_{mn} \hat{b}_n + \tilde{\mathcal{T}}_{mn} \hat{b}_n^\dagger \right\} \end{aligned} \tag{C.6}$$

With this the criteria for bosonic operators can be stated

$$\begin{gathered} \hat{\beta}_n = \hat{\alpha}_n, \quad \hat{b}_n^\dagger = \hat{\alpha}_n^\dagger \\ (\hat{\beta}_n)^\dagger = \hat{\beta}_n^\dagger \\ [\hat{\beta}_n, \hat{\beta}_m^\dagger] = \delta_{nm}, \quad [\hat{\beta}_n, \hat{\beta}_m] = [\hat{\beta}_n^\dagger, \hat{\beta}_m^\dagger] = 0 \end{gathered} \tag{C.7}$$

For the first of the above criteria to be satisfied, the transformations of (C.6) must relate to one another in the following manner

$$\begin{aligned} \hat{\beta}_m^\dagger &= \sum_{n=1}^{N} \left\{ \hat{b}_n^\dagger \mathcal{U}_{nm} + \hat{b}_n \mathcal{V}_{nm} \right\} = \sum_{n=1}^{N} \left\{ \tilde{\mathcal{S}}_{nm} \hat{b}_n + \tilde{\mathcal{T}}_{nm} \hat{b}_n^\dagger \right\} = \hat{\alpha}_m^\dagger \\ \alpha_m &= \sum_{n=1}^{N} \left\{ \tilde{\mathcal{U}}_{nm} \hat{b}_n + \tilde{\mathcal{V}}_{nm} \hat{b}_n^\dagger \right\} = \sum_{n=1}^{N} \left\{ \hat{b}_n^\dagger \mathcal{S}_{nm} + \hat{b}_n \mathcal{T}_{nm} \right\} = \hat{\beta}_m \end{aligned} \tag{C.8}$$

From which it can be inferred

$$\boldsymbol{\mathcal{U}} = \tilde{\boldsymbol{\mathcal{T}}}^T, \ \ \tilde{\boldsymbol{\mathcal{U}}} = \boldsymbol{\mathcal{T}}^T, \ \ \boldsymbol{\mathcal{V}} = \tilde{\boldsymbol{\mathcal{S}}}^T, \ \ \tilde{\boldsymbol{\mathcal{V}}} = \boldsymbol{\mathcal{S}}^T \tag{C.9}$$

The next constraint results from the second criteria

$$\left(\hat{\beta}_m\right)^\dagger = \left(\sum_{n=1}^{N} \left\{ \tilde{\mathcal{U}}_{mn} \hat{b}_n + \tilde{\mathcal{V}}_{mn} \hat{b}_n^\dagger \right\} \right)^\dagger = \sum_{n=1}^{N} \left\{ \tilde{\mathcal{U}}_{mn}^* \hat{b}_n^\dagger + \tilde{\mathcal{V}}_{mn}^* \hat{b}_n \right\} = \sum_{n=1}^{N} \left\{ \hat{b}_n^\dagger \mathcal{U}_{nm} + \hat{b}_n \mathcal{V}_{nm} \right\} = \hat{\beta}_m^\dagger \tag{C.10}$$

Which implies

$$\tilde{\mathcal{U}}^\dagger = \mathcal{U}, \quad \tilde{\mathcal{V}}^\dagger = \mathcal{V} \tag{C.11}$$

The transformation matrices are now

$$\mathcal{A} = \begin{bmatrix} \boldsymbol{\mathcal{U}} & \boldsymbol{\mathcal{V}}^* \\ \boldsymbol{\mathcal{V}} & \boldsymbol{\mathcal{U}}^* \end{bmatrix}, \quad \mathcal{A}' = \begin{bmatrix} \boldsymbol{\mathcal{U}}^\dagger & \boldsymbol{\mathcal{V}}^\dagger \\ \boldsymbol{\mathcal{V}}^T & \boldsymbol{\mathcal{U}}^T \end{bmatrix} \tag{C.12}$$

Note now that $\mathcal{A}' = \mathcal{A}^\dagger$, as was expected for a change of basis.

Finally the third criteria demands

$$\delta_{nm} = [\hat{\beta}_n, \hat{\beta}_m^\dagger] = \left[\mathcal{U}_{nl}^* \hat{b}_l + \mathcal{V}_{nl}^* \hat{b}_l, \hat{b}_k^\dagger \mathcal{U}_{km} + \hat{b}_k \mathcal{V}_{km}\right] = \mathcal{U}_{nl}^* \mathcal{U}_{lm} - \mathcal{V}_{nl}^* \mathcal{V}_{lm} \rightarrow \boldsymbol{\mathcal{U}}^\dagger \boldsymbol{\mathcal{U}} - \boldsymbol{\mathcal{V}}^\dagger \boldsymbol{\mathcal{V}} = \mathcal{I} \tag{C.13}$$

And

$$0 = [\hat{\beta}_n, \hat{\beta}_m] \left[\mathcal{U}_{nl}^* \hat{b}_l + \mathcal{V}_{nl}^* \hat{b}_l, \mathcal{U}_{mk}^* \hat{b}_k + \mathcal{V}_{mk}^* \hat{b}_k\right] \rightarrow \boldsymbol{\mathcal{V}}\boldsymbol{\mathcal{U}}^T - \boldsymbol{\mathcal{U}}\boldsymbol{\mathcal{V}}^T = 0 \tag{C.14}$$

Which is the canonical commutation relation expressed in matrix form.

Now introducing the matrix

$$\boldsymbol{\mathcal{G}} = \begin{bmatrix} \mathcal{I} & 0 \\ 0 & -\mathcal{I} \end{bmatrix} \tag{C.15}$$

It can be seen that (C.13) and (C.14) means the transformation $\mathcal{A}$ satisfies

$$\mathcal{A}^\dagger \mathcal{G} \mathcal{A} = \mathcal{G} \tag{C.16}$$

By noting that $\mathcal{G}^2 = \mathcal{I}$, the above equality is equal to

$$\mathcal{A}^{-1} = \mathcal{G}\mathcal{A}\mathcal{G}, \quad \mathcal{A}\mathcal{G}\mathcal{A}^\dagger = \mathcal{G} \tag{C.17}$$

Which [43] refers to as being $\mathcal{G}$-*paraunitary*. Similarly, by introducing the matrix

$$\mathcal{F} = \begin{bmatrix} 0 & \mathcal{I} \\ \mathcal{I} & 0 \end{bmatrix} \tag{C.18}$$

It follows that

$$\mathcal{F}\mathcal{A}\mathcal{F} = \mathcal{A}^* \tag{C.19}$$

Which is referred to as being $\mathcal{F}$-*canonically consistent*. Now if $\mathcal{A}$ is $\mathcal{F}$-canonically consistent, then so is $\mathcal{G}\mathcal{A}\mathcal{G}$. This motivates the definition of the matrix $\mathcal{B}$

$$\mathcal{B} = \mathcal{G}\mathcal{A}\mathcal{G} \tag{C.20}$$

The two transformation matrix $\mathcal{B}$ and $\mathcal{A}$ therefore follow these relations

$$\mathcal{B} = \mathcal{G}\mathcal{A}\mathcal{G}, \quad \mathcal{B}^{-1} = \mathcal{A}^\dagger$$

$$\mathcal{A} = \mathcal{G}\mathcal{B}\mathcal{G}, \quad \mathcal{A}^{-1} = \mathcal{B}^\dagger \tag{C.21}$$

With the properties of the transformation matrices established, the Hamiltonian in (C.1) can now be canonically diagonalized. First inserting $\mathcal{I} = \mathcal{G}^2$

$$\hat{H} = \boldsymbol{b}^\dagger \mathcal{G} \boldsymbol{M} \boldsymbol{b} \tag{C.22}$$

With $\boldsymbol{M} \equiv \mathcal{G}\boldsymbol{H}$, the transformation matrix $\boldsymbol{B}$ can be found as the eigenvectors of $\boldsymbol{M}$

$$\begin{aligned}\hat{H} &= \frac{1}{2}\boldsymbol{b}^\dagger \mathcal{G}\mathcal{B}\mathcal{B}^{-1}\boldsymbol{M}\mathcal{B}\mathcal{B}^{-1}\boldsymbol{b} = \frac{1}{2}\boldsymbol{b}^\dagger \mathcal{G}\mathcal{B} \begin{bmatrix} \boldsymbol{\omega} & 0 \\ 0 & -\boldsymbol{\omega} \end{bmatrix} \mathcal{B}^{-1}\boldsymbol{b} = \frac{1}{2}\boldsymbol{b}\mathcal{G}\mathcal{B}\mathcal{G} \begin{bmatrix} \boldsymbol{\omega} & 0 \\ 0 & \boldsymbol{\omega} \end{bmatrix} \mathcal{B}^{-1}\boldsymbol{b} \\ &= \frac{1}{2}\boldsymbol{b}^\dagger \mathcal{A} \begin{bmatrix} \boldsymbol{\omega} & 0 \\ 0 & \boldsymbol{\omega} \end{bmatrix} \mathcal{A}^\dagger \boldsymbol{b} = \frac{1}{2}\boldsymbol{\beta}^\dagger \begin{bmatrix} \boldsymbol{\omega} & 0 \\ 0 & \boldsymbol{\omega} \end{bmatrix} \boldsymbol{\beta} = \sum_{n=1}^{N} \hbar\omega_n \left(\hat{\beta}_n^\dagger \hat{\beta}_n + \frac{1}{2} \right)\end{aligned} \tag{C.23}$$

Which completes this treatment of the diagonalizing Bogoliubov transformation. Note that since $\boldsymbol{M}$ is per definition *not* a Hermitian matrix, the diagonalizing eigenvectors are *not* unitary as a result. Diagonalizing $\boldsymbol{M}$ therefore requires inverting the matrix of eigenvectors. This poses a serious problem when the Hamiltonian has a zero mode. As the determinant of the matrix of eigenvectors is given by the product of eigenvalues, a zero mode will imply that $\boldsymbol{B}$ is singular and cannot be inverted, which then implies that $\boldsymbol{M}$ can not be diagonalized. For certain cases a Hamiltonian with zero modes can still be diagonalized with other methods [9, 10]. For the purposes of this project, however, the problem of zero modes was avoided altogether for the transmission line by grounding its endpoints.

Finally, it should also be noted that numerically computing the eigenvectors of $\boldsymbol{M}$ do not necessarily yield the $\boldsymbol{B}$ with a corresponding $\mathcal{A}$ that matches the matrix structure of (C.12). The resulting transformation matrices are therefore *not* $\mathcal{F}$-canonically consistent or $\mathcal{G}$-paraunitary, and the whole algebra applied in the diagonalization in (C.23) no longer holds. This became apparent when an attempt was made to change the basis of a Hamiltonian of oscillators coupled in a chain-like fashion to a star-like fashion with all oscillators connected to a single mode. While the eigenvalues agreed with other diagonalization methods, the couplings between system and bath modes were not the same as the coupling between bath modes and the system. The Hamiltonian had become non-Hermitian. Finding $\mathcal{F}$-canonically consistent and $\mathcal{G}$-paraunitary transformation succeeded for very small systems of around three bath modes with a mix of manual inspection and the diagonalization algorithm of [8], however this could not extended to larger system sizes. The choice was therefore made to remain in a flux-charge whenever possible, as a change of basis can easily be performed using unitary eigenvectors. While finding the correct eigenvectors was not achieved, the Bogoliubov transformation still yielded the correct eigenvalues, which are the ones seen on figure 3.3.5.

Appendix D

Derivation of the dispersion relation for the RWA transmission line

Neglecting the anomalous terms in (3.53) results in the following inverse induction and capacitance matrices

$$\boldsymbol{L}_{\mathrm{RWA}}^{-1} = \begin{bmatrix} \frac{3}{4L} & -\frac{1}{2L} & \\ -\frac{1}{2L} & \frac{3}{4L} & \ddots \\ & \ddots & \ddots \end{bmatrix}, \quad \boldsymbol{C}_{\mathrm{RWA}}^{-1} = \begin{bmatrix} \frac{3}{4C} & -\frac{1}{2C} & \\ -\frac{1}{2C} & \frac{3}{4C} & \ddots \\ & \ddots & \ddots \end{bmatrix} \tag{D.1}$$

Like the capacitively coupled resonator circuits, the RWA has introduced a new coupling to cancel the anomalous processes. As both matrices are now tridiagonal, the dynamical matrix (3.26) of the system is now "quintdiagonal"

$$\boldsymbol{C}_{\mathrm{RWA}}^{-1}\boldsymbol{L}_{\mathrm{RWA}}^{-1} = \frac{1}{4LC}\begin{bmatrix} 10 & -6 & 1 & & \\ -6 & 11 & -6 & 1 & \\ 1 & -6 & 11 & -6 & \ddots \\ & 1 & -6 & \ddots & \ddots \\ & & \ddots & \ddots & \end{bmatrix} \tag{D.2}$$

And the dynamics are thus determined by five unique equations instead of three, one for each boundary, one for the bulk and one for each node next to the boundary. It is worth noting that dismissing the anomalous terms of the Hamiltonian necessitates a new set of interactions with each node's next-nearest neighbor to cancel the initial anomalous terms from their nearest neighbor interactions. With inspiration from the

diagonalization of (4.44), the ansatz of forward and backward propagating waves (4.46) is applied to the bulk equation in the hope of extracting the eigenvalues

$$(\lambda^q - 11)\Psi^q_m = \Psi^q_{m-2} - 6\Psi^q_{m-1} - 6\Psi^q_{m-1} + \Psi^q_{m+2}$$

$$= \left(e^{2iq} + e^{-2iq}\right)\Psi^q_m - 6\left(e^{iq} + e^{-iq}\right)\Psi^q_m = (2\cos 2q - 12\cos q)\Psi^q_m \tag{D.3}$$

Which implies that the dispersion relation is

$$\omega_{\mathrm{RWA}}(\omega) = \frac{\omega_0}{2}\sqrt{11 + 2\cos 2q - 12\cos q} \tag{D.4}$$

Using the discretization of q that was obtained in (4.52), the above dispersion relation matches with the numerical RWA dispersion of (3.3.5). The gapped mass is thus seen to be a result of the nodes of the system including next-nearest neighbor interactions in order to cancel the anomalous terms.

Bibliography

[1] Joachim Ankerhold and Eli Pollak. "Dissipation can enhance quantum effects". In: *Physical Review E* 75.4 (2007), p. 041103.

[2] Mary L Boas. *Mathematical methods in the physical sciences*. John Wiley & Sons, 2006.

[3] Henrik Bruus and Karsten Flensberg. *Many-body quantum theory in condensed matter physics: an introduction*. OUP Oxford, 2004.

[4] Ralf Bulla et al. "Numerical renormalization group for quantum impurities in a bosonic bath". In: *Physical Review B* 71.4 (2005), p. 045122.

[5] Amir O Caldeira and Anthony J Leggett. "Influence of dissipation on quantum tunneling in macroscopic systems". In: *Physical review letters* 46.4 (1981), p. 211.

[6] Amir O Caldeira and Anthony J Leggett. "Quantum tunnelling in a dissipative system". In: *Annals of physics* 149.2 (1983), pp. 374–456.

[7] Herbert B Callen and Theodore A Welton. "Irreversibility and generalized noise". In: *Physical Review* 83.1 (1951), p. 34.

[8] JHP Colpa. "Diagonalization of the quadratic boson hamiltonian". In: *Physica A: Statistical Mechanics and its Applications* 93.3-4 (1978), pp. 327–353.

[9] JHP Colpa. "Diagonalization of the quadratic boson Hamiltonian with zero modes: I. Mathematical". In: *Physica A: Statistical Mechanics and its Applications* 134.2 (1986), pp. 377–416.

[10] JHP Colpa. "Diagonalization of the quadratic boson Hamiltonian with zero modes: II. Physical". In: *Physica A: Statistical Mechanics and its Applications* 134.2 (1986), pp. 417–442.

[11] Alessandro Cuccoli et al. "Quantum thermodynamics of systems with anomalous dissipative coupling". In: *Physical Review E* 64.6 (2001), p. 066124.

[12] Jean-Claude Cuenin and Isroil A Ikromov. "Sharp time decay estimates for the discrete Klein–Gordon equation". In: *Nonlinearity* 34.11 (2021), p. 7938.

[13] Avijit Das et al. “Quantum Brownian motion: Drude and Ohmic baths as continuum limits of the Rubin model”. In: *Physical Review E* 102.6 (2020), p. 062130.

[14] Suman G Das and Abhishek Dhar. “Landauer formula for phonon heat conduction: relation between energy transmittance and transmission coefficient”. In: *The European Physical Journal B* 85 (2012), pp. 1–8.

[15] Richard P Feynman. *Statistical mechanics: a set of lectures*. CRC press, 2018.

[16] George W Ford, John T Lewis, and Robert O’Connell. “Quantum langevin equation”. In: *Physical Review A* 37.11 (1988), p. 4419.

[17] Uri Gavish, Y Levinson, and Yoseph Imry. “Detection of quantum noise”. In: *Physical Review B* 62.16 (2000), R10637.

[18] Steven M Girvin. *Circuit QED: superconducting qubits coupled to microwave photons*. 2014.

[19] Herbert Goldstein, Charles Poole, and John Safko. *Classical mechanics*. 2002.

[20] Pierre Gravel and Claude Gauthier. “Classical applications of the Klein–Gordon equation”. In: *American Journal of Physics* 79.5 (2011), pp. 447–453.

[21] John Bertrand Johnson. “Thermal agitation of electricity in conductors”. In: *Physical review* 32.1 (1928), p. 97.

[22] Alex Kamenev. *Field theory of non-equilibrium systems*. Cambridge University Press, 2023.

[23] Philip Krantz et al. “A quantum engineer’s guide to superconducting qubits”. In: *Applied physics reviews* 6.2 (2019).

[24] Ryogo Kubo, Morikazu Toda, and Natsuki Hashitsume. *Statistical physics II: nonequilibrium statistical mechanics*. Vol. 31. Springer Science & Business Media, 2012.

[25] Lev Davidovich Landau and Evgenii Mikhailovich Lifshitz. *Statistical Physics: Volume 5*. Vol. 5. Elsevier, 2013.

[26] Don S Lemons and Anthony Gythiel. “Paul Langevin’s 1908 paper” On the Theory of Brownian Motion”[” Sur la thiorie du mouvement brownien,” CR Acad. Sci.(Paris) 146, 530-533 (1908)]”. In: *American Journal of Physics* 65 (1997), pp. 1079–1081.

[27] GB Lesovik and R Loosen. “On the detection of finite-frequency current fluctuations”. In: *Journal of Experimental and Theoretical Physics Letters* 65 (1997), pp. 295–299.

[28] Ettore Minguzzi. "Rayleigh's dissipation function at work". In: *European Journal of Physics* 36.3 (2015), p. 035014.

[29] Namiko Mitarai. "Diffusive and Stochastic Processes: Lecture notes". 2023.

[30] Yuli V Nazarov and Jeroen Danon. *Advanced quantum mechanics: a practical guide*. Cambridge University Press, 2013.

[31] Harry Nyquist. "Thermal agitation of electric charge in conductors". In: *Physical review* 32.1 (1928), p. 110.

[32] Jukka P Pekola and Bayan Karimi. "Heat bath in a quantum circuit". In: *arXiv preprint arXiv:2310.01246* (2023).

[33] Jukka P Pekola and Bayan Karimi. "Ultrasensitive calorimetric detection of single photons from qubit decay". In: *Physical Review X* 12.1 (2022), p. 011026.

[34] David M Pozar. *Microwave engineering*. John wiley & sons, 2011.

[35] Edward M Purcell et al. *Electricity and magnetism*. Vol. 2. McGraw-Hill New York, 1965.

[36] Simon Ramo, John R Whinnery, and Theodore Van Duzer. *Fields and waves in communication electronics*. John Wiley & Sons, 1994.

[37] SE Rasmussen et al. "Superconducting circuit companion—an introduction with worked examples". In: *PRX Quantum* 2.4 (2021), p. 040204.

[38] Jun John Sakurai and Jim Napolitano. *Modern quantum mechanics*. Cambridge University Press, 2020.

[39] Samuel Sambursky. *The physical world of late antiquity*. Vol. 825. Princeton University Press, 2014.

[40] Maximilian Schlosshauer. "Quantum decoherence". In: *Physics Reports* 831 (2019), pp. 1–57.

[41] Marlan O. Scully and M. Suhail Zubairy. "Quantum theory of the laser – Heisenberg–Langevin approach". In: *Quantum Optics*. Cambridge University Press, 1997, pp. 362–382.

[42] Daniel D Stancil and Gregory T Byrd. *Principles of superconducting quantum computers*. John Wiley & Sons, 2022.

[43] Hano Omar Mohammad Sura. *Nematic Phase Transitions in J_1-J_2 Square Lattice*. Niels Bohr Institute, Copenhagen University, 2019.

[44] Uwe C Täuber. *Critical dynamics: a field theory approach to equilibrium and non-equilibrium scaling behavior*. Cambridge University Press, 2014.

[45] Uri Vool and Michel Devoret. “Introduction to quantum electromagnetic circuits”. In: *International Journal of Circuit Theory and Applications* 45.7 (2017), pp. 897–934.

[46] Ulrich Weiss. *Quantum dissipative systems (fifth Edition)*. World Scientific, 2021. ISBN: 9789811241499.

[47] YP Zhong et al. “Violating Bell’s inequality with remotely connected superconducting qubits”. In: *Nature Physics* 15.8 (2019), pp. 741–744.